

Electronic Thesis and Dissertation Repository

8-19-2015 12:00 AM

Characterization of fine particle fluidization

Mengqi Han

The University of Western Ontario

Supervisor

Dr. Jesse Zhu

The University of Western Ontario

Graduate Program in Chemical and Biochemical Engineering

A thesis submitted in partial fulfillment of the requirements for the degree in Master of
Engineering Science

© Mengqi Han 2015

Follow this and additional works at: <https://ir.lib.uwo.ca/etd>

Recommended Citation

Han, Mengqi, "Characterization of fine particle fluidization" (2015). *Electronic Thesis and Dissertation Repository*. 3073.

<https://ir.lib.uwo.ca/etd/3073>

This Dissertation/Thesis is brought to you for free and open access by Scholarship@Western. It has been accepted for inclusion in Electronic Thesis and Dissertation Repository by an authorized administrator of Scholarship@Western. For more information, please contact wlsadmin@uwo.ca.

CHARACTERIZATION OF FINE PARTICLE FLUIDIZATION

(Thesis format: Manuscript)

By

Mengqi Han

Graduate Program in Engineering Science
Department of Chemical and Biochemical Engineering

A thesis submitted in partial fulfillment
of the requirements for the degree of
Master of Engineering Science

The School of Graduate and Postdoctoral Studies
Western University
London, Ontario, Canada

© Mengqi Han 2015

ABSTRACT

The major challenge in Geldart group C fine particle fluidization is the cohesive nature of particle properties because of the strong interparticle forces. Nanoparticles as fluidization aids could improve fluidization behavior and reduce the phenomena of channeling and agglomeration. Fundamental studies on fine particle fluidization with nanoparticles were carried out with regard to pressure drop, bed expansion, and minimal fluidization velocity properties. These experiments provided a good base for multilevel analyses in particle size, particle density, nanoparticle concentration etc.

Two pressure drop test methods and two bed expansion test methods were used to characterize the special fluidization behavior of fine particles, compared to Geldart group A particle fluidization. The significant fluidization behavior of high bed expansion and uniform dispersion of group C fine particles with additives indicate a better fluidization with full gas solid contact. A new dimensionless parameter named bed height growth factor (R_G) was introduced to express the particle expansion ability, and R_G is defined as the slope of bed expansion ratio versus gas velocity after minimal fluidization. With increasing additive concentration, increasing bed height growth factor indicated the positive effect of nanoparticles on bed height growth.

Furthermore, flowability of fine particle could be improved by nanoparticles, and powder flow were investigated from dynamic to static, tested by avalanche angle, angle of repose and cohesion.

Keywords

Fine particle fluidization, nanoparticles, pressure drop, bed expansion, minimal fluidization velocity, bed dense phase voidage, flowability, particle size

Acknowledgement

First and foremost, I would like to deeply thank my supervisor Dr. Jesse Zhu for his inspiration and unwavering support throughout the course of this project. I am grateful for the opportunity and experience that he has provided as well as the skills that he has taught me. His trust, patience, encouragement and guidance helped me in all the time of research and writing of this thesis. All his efforts ensured the successful fulfillment of this study, and will be beneficial to my future work.

I am greatly indebted to the helpful staff and other graduate students working under the fluidization and particle technology research group. Graduate students Tian Nan, Zeneng Sun, Xiaoyang Wei, Jiangshan Liu and Zhijie Fu were key elements to the success of this project through their thoughtful criticism and assistance in the laboratory. I am also grateful to Ke Xu who assisted in this project during the times of greatest need.

I wish to take this opportunity to thank Mr. Jianzhang Wen and Mr. Zhi Zhang for their assistance with experimental apparatus and materials. In particular, I wish to thank several of my friends: Ms. Shan Gao, Ms. Danni Bao and Mr. Qingliang Yang for bringing me not only help but also many joys throughout the Master study.

The deepest gratitude goes to my parents, their love, understanding and supports without reservation accompany with me all the time. Thank you for always being the warm harbor of mine, while on the other side of the earth.

Table of Contents

Abstract.....	II
Acknowledgments.....	III
List of Figures.....	VII
1. General Introduction.....	1
1.1 Introduction.....	1
1.2 Objectives.....	2
1.3 Thesis Structure.....	3
1.4 Major Contributions.....	4
Bibliography.....	6
2. Literature Review.....	7
2.1 Powder Properties and Applications.....	7
2.1.1 Particle Size and Size Distribution.....	8
2.1.2 Powder Bulk Density.....	11
2.1.3 Fine Particle Properties and Applications.....	12
2.2 Fluidization of Fine Powder.....	12
2.2.1 Powder Classification by Fluidization Behavior.....	13
2.2.2 Characterization of the Cohesive Particle Fluidization.....	15
2.3 Types of Interparticle Forces.....	16
2.4 Fluidization Aids for Fine Powder.....	18
2.5 Summary and Concluding Remarks.....	19
Nomenclature.....	21
Bibliography.....	23
3. Flow Properties of Fine Powder.....	28

3.1	Experimental Particles and Preparation.....	29
3.2	Cohesion.....	31
3.3	Angle of Repose.....	34
3.4	Avalanche Angle.....	38
3.5	Comparison of Powder Characterization Techniques.....	42
3.6	Conclusions.....	44
	Bibliography.....	46
4.	Experimental Methods and Preliminary Study on Fine Powder Fluidization with Nano-Additives.....	48
4.1	Experimental Apparatus.....	48
4.2	Experimental Methodology.....	50
4.2.1	Pressure Drops and Minimum Fluidization.....	50
4.2.2	Bed Expansion Ratio.....	51
4.3	Difference on Fine Particle Fluidization with or without Nano-additives.....	56
4.4	Discussion on Pressure Drop Test.....	58
4.5	Effect of Particle Size Distribution.....	60
4.6	Conclusions.....	63
	Nomenclature.....	65
	Bibliography.....	66
5	Effects of nanoparticles on Gas-Solid Fluidization.....	68
5.1	Surface Modification by Nanoparticles.....	69
5.2	Fluidization Characterization of Geldart Group C Particles With Nanoparticles.....	71
5.3	Discussion on Bed Height Test.....	75

5.4	Conclusion.....	77
	Nomenclature.....	79
	Bibliography.....	80
6	Further Investigation on Dense Phase Expansion.....	82
6.1	Influence of Nanoparticles on Different Particle Size.....	84
6.2	Bed Collapse Test.....	95
6.3	Discussion.....	86
6.4	Bed Collapse Dense Phase.....	89
6.5	Influence of Gas Velocity on Bed Collapse Test.....	90
6.6	Bed Height Growth Factor.....	92
6.7	Conclusion.....	93
	Nomenclature.....	95
	Bibliography.....	96
7	Conclusions and Recommendations.....	97
7.1	Conclusions.....	97
7.2	Recommendations.....	99
	Curriculum Vitae.....	101

List of Figures

Figure 2.1 Illustration of the concept of equivalent spheres (Malvern Instruments, 2012).....	8
Figure 2.2 Size Distribution with D10, D50, and D90 (Horiba, 2012)	10
Figure 2.3 Geldart Powder Classification (Geldart, 1986)	13
Figure 3.1 Flow chart for preparation of powder samples	30
Figure 3.2 Schematic diagram of shearing strength measurement using a FT4 Powder Rheometer	32
Figure 3.3 Cohesion of glass beads 10 μm blended with nanoparticles	33
Figure 3.4 Cohesion of different particle size (A) Glass beads blended with 16 nm SiO_2 (B) Glass beads virgin particles	34
Figure 3.5 Schematic diagram of a Hosokawa powder tester for angle of repose measurement	35
Figure 3.6 Angle of repose of glass beads blended with R972	37
Figure 3.7 Angle of repose of different particle size	38
Figure 3.8 Schematic of AVA measurement (a) AVA test system (b) Avalanche Angle	39
Figure 3.9 Relationship between avalanche angle and additive concentration	40
Figure 3.10 Relationship between avalanche angle and particle size	42
Figure 3.11 Relationship between AOR, AVA and Cohesion respect to particle size (Glass beads blended with nanoparticles)	43
Figure 3.12 Relationship between AOR, AVA and Cohesion respect to additive concentration (glass beads 10 μm)	44
Figure 4.1 Schematic diagram of the fluidized bed system	49
Figure 4.2 Diagram of pressure drop in fluidized bed (Kunii & Levenspiel, 2013).....	51
Figure 4.3 pressure drop and bed expansion of glass beads 6 μm (Huang, 2009)	54
Figure 4.4 pressure drop and bed expansion of	

glass beads 6 μ m with 0.8%w/w R972	54
Figure 4.5 fluidization characterization of glass beads 10 μ m.....	56
Figure 4.6 fluidization characterization of polyurethane 21 μ m	58
Figure 4.7 comparison of pressure drop test method	59
Figure 4.8 Pressure drop and bed expansion profile of	
glass bead 10 μ m virgin particles	61
Figure 4.9 SEM of glass beads 10 μ m particles.....	62
Figure 5.1 SEM image of glass beads 10 μ m (A) virgin particles	
(B) GB10 blended with 0.8%w/w R972	
(C) GB10 with 0.8%w/w R972 after fluidization	71
Figure 5.2 Fine particle fluidization with nanoparticles compared to Geldart group A	
particles (A) Normalized pressure drop (B) Bed expansion	73
Figure 5.3 Fine particle fluidization with different nanoparticle concentration.....	74
Figure 5.4 The minimal fluidization velocity with different particle	75
Figure 5.5 BER of two test method	77
Figure 6.1 Typical bed collapse test curve	83
Figure 6.2 Bed expansion with nanoparticle of different particle size	85
Figure 6.3 Nanoparticle effect of BER respect to different particle size.....	86
Figure 6.4 Bed collapse test of GB10	87
Figure 6.5 Bed collapse test of GB39 and GB65.....	88
Figure 6.6 Dense phase voidage of 4 kinds of fine particles.....	89
Figure 6.7 GB10 with 0.8%R972 bed collapse test in different gas velocity.....	90
Figure 6.8 Dense phase voidage in different shut down gas velocity.....	91
Figure 6.9 Bed height growth factor of experimental particles.....	93

Chapter 1

General Introduction

1.1. Introduction

Particles have a wide application in many industries, for example in powdered paint and pigments, ceramics, pharmaceuticals, chemical and material industries. The significance of particle technology is apparent in that approximately one-half of the products in the chemical industry and at least three-quarters of the raw materials are in granular (Nedderman, 2005).

With vast applications in industries, particles of a mean diameter less than 30 μm are usually referred to as fine particles (Zhu, 2003). Fine particles gradually became desirable in some industries in recent years because of their special characteristics such as large specific surface area and small size, leading to various advantages. However, at the same time, their poor flow properties also challenge applications of fine powders in terms of processing. The inherent cohesiveness of these particles due to relatively strong interparticle forces makes them very difficult to fluidize (Valverde, Castellanos, Mills, & Quintanilla, 2003).

Fluidization occurs when particulate materials are suspended in an upflowing fluid phase. There are many factors affecting powder fluidization quality: uniform and extensive gas-solid contact, good solids mixing leading to uniform temperature throughout the bed high mass and heat transfer rates, easy solids handling etc (Zhu, 2003). The particles that are suitable for fluidization range from sub-microns to several millimeters, with increasing difficulty in fluidization as particle size decreases. When such fine particles are subject to fluidization, they tend to form channels and agglomerates (Geldart, 1972).

Many measures have been taken to improve the fluidization of fine particles, which called fluidization aids. Most of those measures lend extra energy into the system, to help break up the agglomerates, such as mechanical and acoustic vibration, mechanical stirring, and magnetic and electrical field disturbance. Other measures approach the problem by reducing the surface force of the particles, such as surface adsorption and modifications, or adding larger of finer particles as flowing agents.

One of the widely used flow aids are flow additives which modify the surface of fine particles so that the interparticle forces decrease and the flow properties of fine powder are thus improved. However, the mechanism of the flow additives is still not very clear, and needs further study (Huang, 2009). The operating condition for the flow additives to improve flow properties depends on the properties of the primary powders. With the assistance of flow aids, fine powders behave with improved flowability but somehow differ from coarse powders.

1.2. Objectives

Although numerous previous research on fine particle fluidization were studied, the fundamentals such as bed expansion and pressure drop profile, especially when the nanoparticles were added in the fluidization, should be investigated more and the fluidization behavior also need to be characterized. In addition, further study is needed to elucidate the mechanisms governing the operation of nanoparticles in the improving fluidization quality and flowability of fine particles. Therefore, the present study focuses on the fine particle fluidization with nanoparticles aims to attend the following objectives:

- 1) To investigate the flowability of fine particle with nanoparticles as a flow conditioner,

from static to dynamic.

- 2) To examine the fine particle fluidization behavior of Geldart groups C with and without nanoparticles, and influence of fine particle size management on fluidization.
- 3) To make a comprehensive and parametric investigation on the effect of nanoparticles on fluidization behavior of fine particles, compared to Geldart group A particles.
- 4) To systematically study the fine particle fluidized bed height behavior and detailed study the dense phase bed expansion of fine particles.

1.3. Thesis Structure

This thesis contains seven chapters and follows the “Manuscript” format as outlined in the Thesis Regulation Guide by the faculty of Graduate Studies (FGS) of The University of Western Ontario. It is organized in the following structure.

- Chapter 1 gives a general introduction to the backgrounds of the fine particle fluidization technology and renders the research problems. The research objectives and the thesis structure as well as the major contribution of the present work are also stated.
- Chapter 2 provides a detailed literature review about particle properties and applications, as well as the current status and potential application of the fine particle fluidization technology. Room for future study is suggested.
- Chapter 3 discusses the influence of additive concentration to improving powder

flowability, from static to dynamic. The relationship of several flow properties are employed and compared, leading to a better understanding of these characterization techniques.

- Chapter 4 presents a preliminary study on fine powder fluidization with and without nanoparticles, two pressure profile test method are included, the previous mechanisms of flow additives are examined and the fluidization behavior of fine particles are reported.
- Chapter 5 provide the results of a comprehensive and parametric investigation on the fluidization behavior of fine particles with different nano-additive concentrations, respectively. The possible roles of additive in fluidization of Geldart groups C and A particles are studied.
- Chapter 6 continues exploring the fluidization behavior on bed height, including the bed expansion, bed collapse and a novel “bed height growth factor”, the estimation and validity of this new fluidization characteristic factor are discussed.
- Chapter 7 summarizes the general conclusions of this work, and gives a list of recommendations for the future work.

1.4. Major Contributions

The present study explores several aspects of flow and fluidization of fine powders. The major contributions can be summarized as follows:

- As flowability from static to dynamic can't perfectly match to each other, a thorough analysis on powder flowability has been provided. The role of nanoparticle to improve

fine particle fluidization not equivalent to powder flow, especially for the different type of particles.

- Comprehensive and parametric investigations on the fluidization behavior of fine particles with and without nanoparticles have been conducted. The effects of flow additives on fine powder fluidization are comprehensively examined. The representative particles in the range of fine particle size describes the obviously influence of nanoparticles. The comparative study on Geldart groups C with additives and group A particles are originally explored.
- A special characterization on bed expansion improvement of fine particle fluidization has been discussed. The bed collapse has been illustrated in details to express dense phase bed expansion, as the most welcome state in fluidization occurs which is the high and uniform bed expansion, which means the extensive gas-solid contact, good solids mixing leading to uniform temperature throughout the bed high mass and heat transfer rates. A novel bed height growth factor also has been suggested in future research works.

Bibliography

- Geldart, D. (1972). The effect of particle size and size distribution on the behaviour of gas-fluidised beds. *Powder Technology*. [http://doi.org/10.1016/0032-5910\(72\)83014-6](http://doi.org/10.1016/0032-5910(72)83014-6)
- Huang, Q. (2009). Flow and fluidization properties of fine powders, *Ph.D.* <http://ezproxy.aut.ac.nz/login?url=http://search.proquest.com/docview/305111253?accountid=8440>
- Nedderman, R. M. (2005). *Statics and kinematics of granular materials. Annals of Physics* (Vol. 54).
- Valverde, J. M., Castellanos, A., Mills, P., & Quintanilla, M. A. S. (2003). Effect of particle size and interparticle force on the fluidization behavior of gas-fluidized beds. *Physical Review. E, Statistical, Nonlinear, and Soft Matter Physics*, 67(5 Pt 1), 051305. <http://doi.org/10.1103/PhysRevE.67.051305>
- Zhu, J. (2003). Fluidization of fine powders. *Granular Materials: Fundamentals and Applications*, 270–295. <http://doi.org/10.1007/978-94-007-5587-1>

Chapter 2

Literature Review

“A Particle is defined as a small, discretely identifiable entity that has an interface with the surrounding environment or has a separate domain with respect to the continuous medium” (*Particle Technology and Applications*, 2012). Solid particles are often of great interest in the chemical process industry, mineral processing, pharmaceutical production and energy-related processes, etc. Distinguishing an assembly of particles, powder consists of a solid in a discontinuous state, that is, there are no material bonds between the individual pieces. The particle size is generally considered to extend from sizes as large as 1 mm to sizes of the order of nanometers (Arai, 1996). Although a general agreement to classify a powder by size is not yet available, particles of a mean diameter less than 30 μm are usually referred to as fine particles whose applications in industries are vast. Particle with a diameter less than 10 μm are called superfine particles, which can be further classified as: micron particles (1~10 μm), sub-micron particles (0.1~1 μm), nanoparticles (1~100 nm) and molecular cluster (<1 nm) (Ichinose, Ozaki, & Kashu, 2012).

2.1 Particle Properties and Applications

Particle technology has already been practiced in a variety of forms and applications throughout the world over the course of human history (*Particle Technology and Applications*, 2012). Human produced many kinds of powders to improve their daily life, such as pigments, fertilizers, cements, industrial chemicals, detergents, pharmaceuticals and food. The significance of particle technology is apparent in the approximately one-half of the products in the chemical industry and at least three-quarters of the raw materials are in granular form (Nedderman, 2005). As the important widely application in

industry, particle and their properties is necessarily studied in this work as follow.

2.1.1. Particle Size and Size Distribution

Particle size is one of the fundamental characteristic for a powder as a discrete solid, it influences many properties of particulate materials and is a valuable indicator of quality and performance (Horiba, 2012). Particle size has a direct influence on material properties such as reactivity or dissolution rate, stability in suspension, appearance and flowability (Malvern Instruments, 2012). In this work particle size is directly related to powder flowability and fluidization quality.

Particles are 3-dimensional object, unless they are perfect spheres, they cannot be fully described by a single dimension such as a radius or diameter. In order to simplify the measurement process, it is often convenient to define the particle size using the concept of equivalent spheres. In this case the particle size is defined by the diameter of an equivalent sphere having the same property.

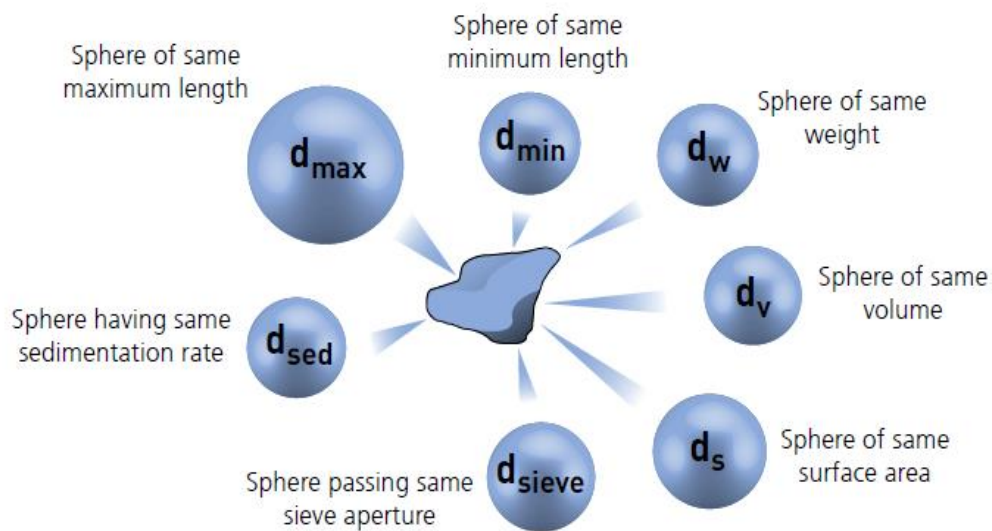


Figure 2.1 Illustration of the concept of equivalent spheres (Malvern Instruments, 2012)

Whatever measure of particle size is chosen, it is very unlikely that all of the particles will have the same size unless some industrial processes aim to produce uniform particles. Normally, there is a wide range of particle size, particularly when the powder has been produced by crushing a coarser form. Generally, the particle size distribution of a powder has to be measured to better understand the effects of particle size on powder flow behaviors.

When reporting a particle size distribution the most common format used even for image analysis systems is equivalent spherical diameter on the x axis and percent on the y axis. It is only for elongated or fibrous particles that the x axis is typically displayed as length rather than equivalent spherical diameter (Horiba, 2012).

Particle size distribution is a range of values, used to describe the size of a group of particles. The average size of the particles does not accurately describe the size distribution of a sample of powders. A better approach is to describe the median size of the particles as well as the width of the distribution. The median, called the D50, is the particle diameter of which 50% by volume of the powder is smaller. The width of the distribution can be described using the span. The span is defined using the following equation:

$$\text{Span} = \frac{D_{90} - D_{10}}{D_{50}}$$

where D10 is the particle diameter of which 10% by volume of the powder is smaller, and D90 is the particle diameter of which 90% by volume of the powder is smaller. Figure 2.2 shows a size distribution and a representation of the three values D10, D50, and D90.

Carr (Carr, 1965) has proposed uniformity of the size distribution as one flow index to characterize powder flow properties. In general, a narrower particle size distribution

indicates better flow properties.

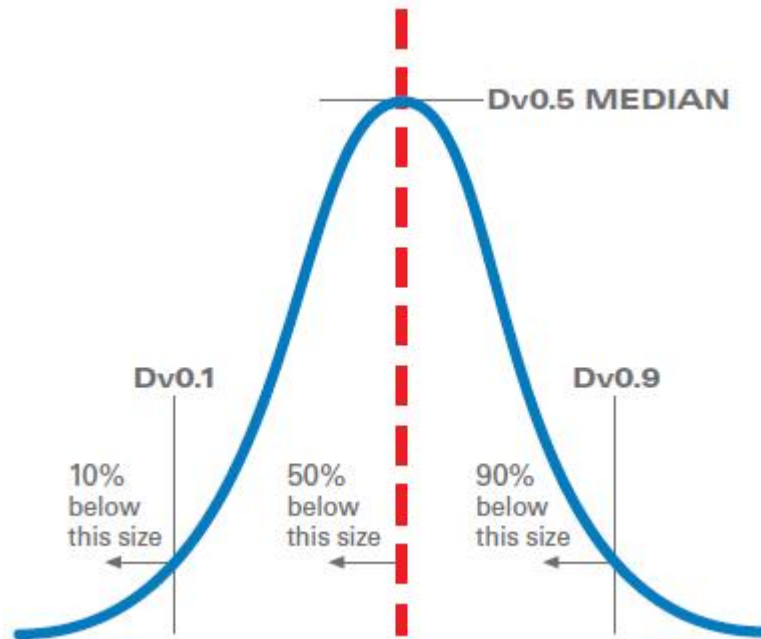


Figure 2.2 Size Distribution with D10, D50, and D90 (Horiba, 2012)

Particle size, and particle size distribution, both play significant roles in flowability (as will be detailed in Section 3), and other properties, such as bulk density, angle of repose, and compressibility of bulk solids. Even a small change in particle size can cause significant alterations in the resulting flowability. Reduction in particle size often tends to decrease the flowability of a given granular material due to the increased surface area per unit mass (Fitzpatrick, Iqbal, Delaney, Twomey, & Keogh, 2004). Particle size also plays an important role in the compressibility of powders. An increase in particle size generally leads to an increase in compressibility (and thus volume reduction) (Yan & Barbosa-Canovas, 1997). The smaller the particle size and greater the range of particle sizes, the greater the cohesive strength, and lower the flow rate (MARINELLI & CARSON, 1992). Reduction in size increases the contact area between the particles, thereby increasing the cohesive forces.

2.1.2. Particle Bulk Density

Three different densities are used to characterize particles: the skeletal density characterizes the solid material from which the particles are made, the apparent particle density accounts for any pores within the particles and the bulk density refers to the powder formed by particles in storage (Briens, 2002).

The bulk density of a powder is the ratio of the mass of an untapped powder sample and its volume including the contribution of the inter-particulate void volume. Hence, the bulk density depends on both the density of powder particles and the spatial arrangement of particles in the powder bed. It can be obtained from the particle density and the voidage ε , which is the volume fraction of the bulk powder occupied by the voids:

$$\rho_b = (1 - \varepsilon)\rho_p + \varepsilon\rho_g \quad (2.1)$$

Where ρ_p and ρ_g are particle density and the density of the interstitial gas in the powder.

The powder bulk density can be in principle measured by filling a vessel of known volume with a powder and then measuring the weight difference between the empty and full vessel. However, if this is attempted, a range of bulk densities can be obtained depending on the manner in which the vessel is filled. Generally, two extreme conditions are used as reference points: loose packing gives the minimum bulk density (maximum possible voidage) and dense packing gives the maximum bulk density (minimum possible voidage); both are based on random packing (Abdullah & Geldart, 1999; Geldart, 1986). Increases in bulk density have been observed when conditioners are added (Peleg & Mannheim, 1973), which results in modification of density via lowering the inter-particle interactions. Bulk density of powders has also been observed to decrease with an increase in the particle size as well as with an increase in equilibrium relative humidity (Yan & Barbosa-

Canovas, 1997).

2.1.3. Fine Particle Properties and Applications

Fine particle is often defined as the particle diameter less than $30\mu\text{m}$, also called cohesive particles. As they are very small and cohesive, generally show poor flow properties in all kinds of powder handling processes, such as arching during silo discharge, non-smooth transportation, channeling and partial fluidization in a fluidized bed and clumping on equipment. However, fine particles also have many advantage properties different from those of the solid, typical of which are: (Ichinose et al., 2012)

- 1) Large surface area per gram weight: heat or material exchange membranes.
- 2) Thin, uniform surface layer : auxiliary combustion agent for rockets
- 3) Stepped surface: high performance, high speed catalysts (reaction facilitated by large number of active points).

Generally, a powder of a smaller size consists of more finely divided solids and has more discontinuous surfaces. As a consequence, the benefit of fine particles gradually make many applications desirable in various industries.

2.2. Fluidization of Fine Powder

Fluidization as one of the popular fine particle applications, always described as an operation through which fine solids are transformed into a fluid like state through contact with a gas or liquid. Under the fluidized state, the gravitational force on granular solid particles is offset by the fluid drag on them. Thus the particles remain in a semi-suspended condition and the gas-solid suspension displays characteristics similar to those of liquid.

2.2.1. Powder Classification by Fluidization Behavior

By investigating the fluidization behaviors of different particles, in 1973 Geldart classified gas-solid fluidization into four groups, group A (aeratable), group B (bubble-ready or sand-like), group C (cohesive), and group d (spoutable), in term of their particles size and density, also the fluidizing behavior. The classification is given in Figure 2.3.

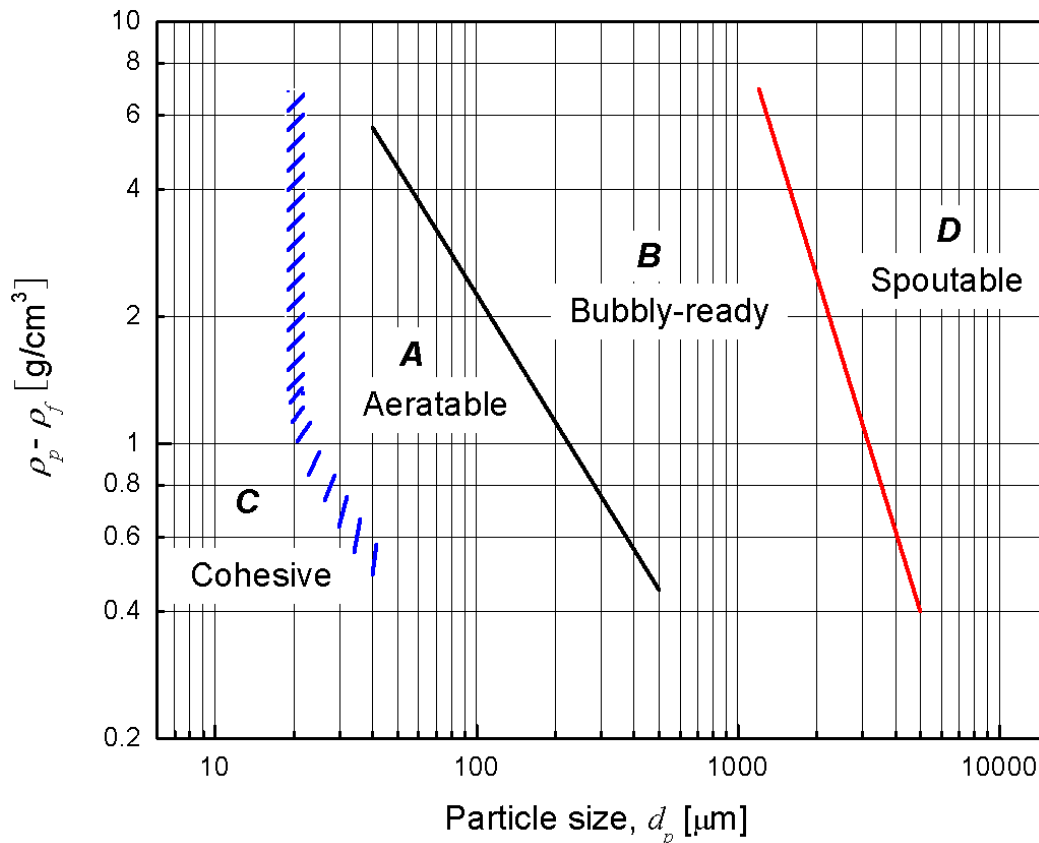


Figure 2.3 Geldart Powder Classification (Geldart, 1986)

Group A is also called aeratable powder, as it could be fluidized well and experiences a period of uniform bed expansion when the superficial gas velocity is beyond the minimal fluidization velocity (U_{mf}). A bubble starting point is eventually reached when the gas velocity exceeds the minimum fluidization velocity and reaches the minimum bubbling velocity (U_{mb}). The particle size of Group A powder is usually in the range of 25-30 μm to about 150-200 μm . Fluid cracking catalysts (FCC) are typical examples.

Group B particles are referred to as bubble-ready or sand-like powder. The particle size range is normally from 150-200 μm to 700-900 μm . The main materials like sand, ore, glass easily goes directly to bubbling fluidization as soon as the gas velocity reaches U_{mf} . In contrast to group A powder, bubbles form in this type of powder at the starting point ($U_{mf}=U_{mb}$) of fluidization and there is actually no particulate fluidization observed.

Group D powders are the largest, of the order 700-900 μm to several millimeters. At higher gas rates the excess gas escapes along bubble rains, which coalesce easily into vertical channels through which particles are swept upwards causing some unstable operation. Group D particles are more suitable for spouted beds and are called spoutable particles.

Group C particles which are in any way cohesive belong in this category, so is also known as cohesive powder. The particle size is almost smaller than 25-40 μm in diameter. The cohesive nature of group C powders comes from the fact that when the particle sizes become smaller, the relative magnitude of the interparticle forces increases. Such strong interparticle forces make the individual particles stick together and form agglomerates that can lead to severe agglomeration, channeling, rat-holing or even complete de-fluidization. Generally, normal fluidization of these powder without any flow aids is very difficult.

The criterion of Geldart scheme, though very qualitative, is accepted worldwide by researchers in the field of particle technology. An empirical criterion, called Hausner ratio, HR (the ratio of tapped to aerated bulk density of the particles), was proposed as an easily available index for characterizing the fluidization quality of particles by (Geldart & Wong, 1985). Also, an experimental method has been proposed by (Bai, D., Grace, J.R. and Zhu,

1999) for distinguishing group C particles from other groups based on the dynamic pressure signals from the bed collapse tests. It was found that the pressure signals for group C particles obviously had a higher dominant frequency, smaller fluctuation and less chaotic nature than those obtained from groups A particles. (Heqing, 1991) identified group C powders through the angle of repose (AOR). It was assumed that particles with $AOR > 40^\circ$ could be classified as group C powders.

2.2.2. Characterization of the Cohesive Particle Fluidization

The basic characteristic of fine particles is usually described as cohesive and difficult to fluidize due to the strong interparticle forces (Baerns, 1966; Geldart, Harnby, & Wong, 1984; Geldart & Wong, 1985; Geldart, 1972, 1973). For cohesive particles in fluidization, the particle bed often exhibits severe channeling, rat-holing and agglomeration, resulting in very poor gas-solid contact with most of the bed areas not fluidized at all rather than a smooth fluidization.

Channeling. As one of the important cohesive particle fluidization characteristics, channeling often occurs when the superficial gas velocity is low. Gas passes up through voids extending from the distributor up to the bed surface then channeling happens. The vertical channels may move across the bed time to time, resulting in the bed de-fluidization. Besides channels, cracks of different orientations, length and tortuosity can also be observed at low velocities (Iyer & Drzal, 1989). With increasing gas velocity, larger channels, so called “rat holes”, may form for some extremely cohesive particles (Mori, 1990; Morooka, Kusakabe, Kobata, & Kato, 1988; Wang, Kwauk, & Li, 1998). Fundamental studies on the formation mechanisms are still quite rare.

Agglomeration. Group C particles inside a fluidized bed may exist three forms: single

particles, natural agglomerates and fluidized agglomerates (Hua, Hu, & Li, 1994; Pacek & Nienow, 1990). Natural agglomerates as the name implies, means that fine particles tend to form spherical agglomerates in natural state, due to cohesiveness when kept in a heap, stored in a vessel, or while being transferred. Another type of agglomerates also forms when the bed is fluidized (Chaouki, Chavarie, Klvana, & Pajonk, 1985).

2.3. Types of Interparticle Forces

Powder fluidization is the result of a balance between hydrodynamic forces on the hand and gravitational and interparticle (or cohesion) forces on the other. Their overall magnitude determines whether a powder can be classified according to type A, B, C or D behavior following Geldart classification (Visser, 1989a). So that the particles are likely to be in free-floating state provided that the interparticle forces are minimum. There are three types of interparticle forces, the Van der Waals force, the Capillary force and the electrostatic force, which make the powders more difficult to fluidize.

Van Der Waals Force. The Van der Waals force previously named as the London force and the dispersion force (Hamaker, 1937), is the dominant interaction force between particles in a powder as well as in a fluidized bed. It's a collective term taken to include the dipole/dipole, dipole/non-polar and non-polar/non-polar forces arising between molecules (Seville, Willett, & Knight, 2000). This force always exists and is usually the largest interparticle force among the three types. Van der Waals forces become noticeable only when the particles are very close (e.g. 0.2 to 1nm) and are small enough, e.g. 30 μm or less. Van der Waals force may be estimated using the following equation for spherical particles.

$$F_{VW} = \frac{AR}{12H^2}$$

Where R = Radius of spherical particles.

A = Hamaker coefficient.

H = Separation distance.

Surface roughness, geometrical structure and possible deformation of the individual particles can significantly change the Van der Waals force.

Electrostatic Force. Particulate system exhibits charging as a result of particle-particle and particle-wall collision. The particle-wall collision is predominant for two-dimensional bed and fine particles. The positively and negatively charged particles are present and there is some evidence that the air stream may hold a balance of charge. During fluidization, strong electrostatic forces are likely to be formed in bed because of dielectric particles. The charges may alter the fluidization characteristic and leads to increased pressure drops, decreased bed expansion, channeling and even complete de-fluidization (Geldart, 1986).

To eliminate electrostatic effects, different techniques have been adopted: the use of humid air (60 to 70% RH) has been shown to increase the conductivities of insulators. The charges produced in the fluidized bed are thus neutralized or conducted to earth. Electrically conducting plastics and transparent metallic coatings are commercially available. Anti-static sprays may be added periodically or continuously to the fluidizing gas upstream from the distributor.

Capillary Force. At high humidity (> 65%), capillary force coming from the fluid condensation in the gap between the particles in close contact may take place resulting in capillary force (Visser, 1989b). If a liquid of low viscosity forms a bridge between two particles, a force F_H acts between them consisting of two components, the surface tension force F_R , and a force F_P due to the difference of the pressure outside and inside the bridge.

$$F_H = F_R + F_P$$

The surface tension force F_R always brings about an attraction; a capillary pressure P_K can

only contribute a positive component to the adhesion force, if it produces a pressure deficiency within the bridge. The influence of gravity may be neglected for particle sizes less than one millimeter (Schubert, 1984).

2.4. Fluidization Aids for Fine Powder

As the strong interparticle forces occur in fine powder fluidization, people have already found several methods to improve the fluidization quality, e.g. many types of vibrators, aerators and flow additives. These measures are collectively called fluidization aids. Despite different design principles and applications, overall the flow aids can be divided into 2 categories: one is to introduce external energy into the system, to break up the agglomerates, such as mechanical and acoustic vibration, mechanical stirring, and magnetic and electrical field disturbance (Barletta, Donsi, Ferrari, Poletto, & Russo, 2008; MORI, 1990; Xie, 1997; Zhu, J; Zhang, 2004). Other measures approach the problem by reducing the surface force of the particles, such as surface adsorption and modifications, or adding larger or finer particles as flowing agents.

The addition of finer particles as flow conditioners can improve the fluidization quality of fine particles, nanoparticles have been widely used for a long time to adjust the flow properties. Dutta & Dullea, 1991 mixed a small amount of nanoparticles such as alumina (29 nm) or aerosil 200 (12 nm) into group C powders and found a significant reduction in the cohesiveness of the powders. Although it is well known that the fluidization quality of cohesive particles can be greatly improved by adding finer particles as flow conditioners, it is still controversial about the operative mechanism through which the flow conditioners are effective. According to the London van der Waals theory (Krupp, 1967), when the van der Waals force dominates over the interparticle cohesive forces, the magnitude of the interparticle forces decreases sharply with the separation distance between two particles.

Thus, in most of the previous studies, it has been generally believed that the flow-conditioner particles reduce the interparticle forces by acting as a physical barrier between the host particles, which may be called the spacer mechanism (Lauga, Chaouki, Klvana, & Chavarie, 1991; Visser, 1989a; Zhou & Li, 1999). However, some researchers questioned about the above mechanism and proposed different mechanisms such as acting as lubricants to reduce friction between host particles (Hollenbach, Peleg, & Rufner, 1983; Kono, Huang, Xi, & Shaffer, 1989), and acting as neutralizers of electrostatic charge (Dutta & Dullea, 1991). Therefore, further study is needed to elucidate the mechanism governing the operation of the flow conditioners.

2.5. Summary and Concluding Remarks

Particle technology have already been used in a variety of forms and applications, such as pigments, fertilizers, cements, industrial chemicals, detergents, pharmaceuticals and food, up to approximately 70% of raw materials are in granular form. Fluidization as one of the preferred mode handling particles, has to be brought into good contact for physical and chemical processing. In 1973, Geldart input a famous powder classification, in term of the different fluidization behavior. The four group powder is: Group A (aeratable), group B (bubble-ready), group C (cohesive) and group D (spoutable). Group C particles are very fine, which diameter is smaller than 30 μm , the strong interparticle forces directly result in de-fluidization. The individual fine particles often sling to each other and therefore form agglomerates, which can lead to severe agglomeration, channeling and even de-fluidization. In order to improve fine particles fluidization, several measures referred to as fluidization aids have been developed by introducing external energy and optimizing surface properties. These included mechanical and acoustic vibration, mechanical stirring, gas absorption and adding coarser or finer particles as flow conditioners.

Although flow additives have been known to effectively improve fluidization of fine particles, the fundamentals of their fluidization with nanoparticles have rarely been the subject of study, such as their pressure drop and bed expansion profile, minimal fluidization velocity and comparative study with fluidization of group A particles, the mechanism of improved flow properties is still not very clear. In addition, a further study exists in this subject such as the agglomerate size, interparticle force measurements and particle size management. Therefore, more fundamental and comprehensive studies on fine particle fluidization with nanotechnology are necessary.

Nomenclature

A	Hamaker Coefficient, [J]
AOR	Angle of Repose, [°]
D10	Particle sizes where 10% of particles (in number or volume or weight) have smaller size than it, [m]
D50	Powder median diameter, the particle size where 50% (in number or volume or weight) have smaller size than it, [m]
D90	Particle sizes where 90% of particles (in number or volume or weight) have smaller size than it, [m]
F _H	Capillary force at high humidity (>65% RH), [N]
F _P	A force due to pressure differences of outside and inside the bridge between two particles, [N]
F _R	Surface tension force, [N]
F _{VW}	Van der Waals force between two solid particles, [Pa]
H	Separation distance between two particles, [m]
HR	Hausner ratio, [-]
R	Radius of spherical particles, [m]
RH	Relative humidity
U _{mb}	Minimum bubbling gas velocity, [m/s]
U _{mf}	Minimum fluidization gas velocity, [m/s]

Greek letters

ρ_b	Powder bulk density. [kg/m ³]
ρ_g	Gas density, [kg/m ³]

ρ_p	Particle density, [kg/m ³]
ε	Powder voidage, [-]

Bibliography

- Abdullah, E. C., & Geldart, D. (1999). The use of bulk density measurements as flowability indicators. *Powder Technology*, *102*(2), 151–165.
[http://doi.org/10.1016/S0032-5910\(98\)00208-3](http://doi.org/10.1016/S0032-5910(98)00208-3)
- Arai, Y. (1996). *Chemistry of Powder Production*. Springer Science & Business Media.
Retrieved from <https://books.google.com/books?hl=en&lr=&id=6Bgew6-rNgwC&pgis=1>
- Baerns, M. (1966). Effect of interparticle adhesive forces on fluidization of fine particles. *Industrial & Engineering Chemistry Fundamentals*. Retrieved from
<http://pubs.acs.org/doi/abs/10.1021/i160020a013>
- Bai, D., Grace, J.R. and Zhu, J. (1999). Characterization of gas fluidized beds of group C, A and B particles based on pressure fluctuations. *The Can.J.Chem.Eng.*, *77*, 319-324.
- Barletta, D., Donsì, G., Ferrari, G., Poletto, M., & Russo, P. (2008). The effect of mechanical vibration on gas fluidization of a fine aeratable powder. *Chemical Engineering Research and Design*, *86*(4), 359–369.
<http://doi.org/10.1016/j.cherd.2007.10.002>
- Bridgwater, J. (1995). Particle technology. *Chemical Engineering Science*, *50*(24 pt B), 4081–4089. [http://doi.org/10.1016/0009-2509\(95\)00225-1](http://doi.org/10.1016/0009-2509(95)00225-1)
- Briens. (2002). Chapter 1 Characterization Of Individual Particles, 1–48.
- Carr, J. (1965). Classifying flow properties of solids. *Chemical Engineering*, *72*(3), 69–72.
Retrieved from https://www.engineeringvillage.com/blog/document.url?mid=c84_1cf782f941d80c1cM6c7919817173212&database=c84
- Cassell, A. M., Raymakers, J. A., Jing Kong, & Hongjie Dai. (1999). Large scale CVD synthesis of single-walled carbon nanotubes. *Journal of Physical Chemistry B*, *103*(31). [http://doi.org/10.1021/jp990957sCCC:\\$18.00](http://doi.org/10.1021/jp990957sCCC:$18.00)
- Chaouki, J., Chavarie, C., & Klvana, D. (1986). Study of Selective Hydrogenation of Cyclopentadiene on a Fluidized Cu/Al₂O₃ Aerogel. *Canadian Journal of Chemical Engineering*, *64*(3), 440–446. Retrieved from
http://www.engineeringvillage.com/blog/document.url?mid=cpx_2019456&database=cpx

- Chaouki, J., Chavarie, C., Klvana, D., & Pajonk, G. (1985). Effect of interparticle forces on the hydrodynamic behaviour of fluidized aerogels. *Powder Technology*, 43(2), 117–125. [http://doi.org/10.1016/0032-5910\(85\)87003-0](http://doi.org/10.1016/0032-5910(85)87003-0)
- Dutta, A., & Dullea, L. (1991). Effects of external vibration and the addition of fibers on the fluidization of a fine powder. *AIChE Symp. Ser.* Retrieved from https://scholar.google.ca/scholar?hl=en&q=effect+of+external+vibration+and+the+addition+of+fibers+on+the+fluidization+of+a+fine+powder&btnG=&as_sdt=1%2C5&as_sdtpr=#0
- Fitzpatrick, J. ., Iqbal, T., Delaney, C., Twomey, T., & Keogh, M. . (2004). Effect of powder properties and storage conditions on the flowability of milk powders with different fat contents. *Journal of Food Engineering*, 64(4), 435–444. <http://doi.org/10.1016/j.jfoodeng.2003.11.011>
- Geldart, D. (1972). The effect of particle size and size distribution on the behaviour of gas-fluidised beds. *Powder Technology*. [http://doi.org/10.1016/0032-5910\(72\)83014-6](http://doi.org/10.1016/0032-5910(72)83014-6)
- Geldart, D. (1973). Types of gas fluidization. *Powder Technology*, 7(5), 285–292. [http://doi.org/10.1016/0032-5910\(73\)80037-3](http://doi.org/10.1016/0032-5910(73)80037-3)
- Geldart, D. (1986). Gas fluidization technology. Retrieved from <http://www.osti.gov/scitech/biblio/6808024>
- Geldart, D., Harnby, N., & Wong, A. C. (1984). Fluidization of cohesive powders. *Powder Technology*. [http://doi.org/10.1016/0032-5910\(84\)80003-0](http://doi.org/10.1016/0032-5910(84)80003-0)
- Geldart, D., & Wong, A. C. Y. (1985). Fluidization of powders showing degrees of cohesiveness—II. Experiments on rates of de-aeration. *Chemical Engineering Science*. [http://doi.org/10.1016/0009-2509\(85\)80011-7](http://doi.org/10.1016/0009-2509(85)80011-7)
- Hamaker, H. C. (1937). The London—van der Waals attraction between spherical particles. *Physica*, 4(10), 1058–1072. [http://doi.org/10.1016/S0031-8914\(37\)80203-7](http://doi.org/10.1016/S0031-8914(37)80203-7)
- Heqing, Z. (1991). RESEARCH ON FLUIDIZATION CHARACTERISTICS OF GROUP C POWDERS. *The Chinese Journal of Process Engineering*. Retrieved from http://en.cnki.com.cn/Article_en/CJFDTOTAL-HGYJ199103009.htm
- Hollenbach, A., Peleg, M., & Rufner, R. (1983). Interparticle surface affinity and the bulk properties of conditioned powders. *Powder Technology*. Retrieved from

<http://www.sciencedirect.com/science/article/pii/0032591083850268>

Horiba. (2012). a Guidebook To Particle Size Analysis, 1–29.

Hua, B., Hu, L., & Li, C. (1994). Process of collapse and expansion of ultrafine powder fluidized bed. *Hua Dong Li Gong Da Xue/Journal of East China University of Science and Technology*, v 20, n 3, 290 – 294.

Ichinose, N., Ozaki, Y., & Kashu, S. (2012). *Superfine Particle Technology*. Springer Science & Business Media. Retrieved from <https://books.google.com/books?id=IYjbBwAAQBAJ&pgis=1>

Iyer, S., & Drzal, L. (1989). Behavior of cohesive powders in narrow-diameter fluidized beds. *Powder Technology*. Retrieved from <http://www.sciencedirect.com/science/article/pii/0032591089800166>

Kim, Y. K., Lee, K. Y., Kwon, O. K., Shin, D. M., Sohn, B. C., & Choi, J. H. (2000). Size dependence of electroluminescence of nanoparticle (rutile-TiO₂) dispersed MEH-PPV films. *Synthetic Metals*, 111-112. [http://doi.org/10.1016/S0379-6779\(99\)00348-3](http://doi.org/10.1016/S0379-6779(99)00348-3)

Kono, H., Huang, C., Xi, M., & Shaffer, F. (1989). The effect of flow conditioners on the tensile strength of cohesive powder structures. *AIChE Symp. Ser.* Retrieved from https://scholar.google.ca/scholar?q=effect+of+flow+conditioners+on+the+tensile+strength+of+cohesive+powder+structures&btnG=&hl=en&as_sdt=0%2C5#1

Kono, H., Matsuda, T., Huang, C., & Tian, D. (1990). Agglomeration cluster formation of fine powders in gas-solid two phase flow. *AIChE Symp. Ser.* Retrieved from https://scholar.google.ca/scholar?q=agglomeration+cluster++formation+of+fine+p owders+in+gas-solid+two+phase+flow&btnG=&hl=en&as_sdt=0%2C5#0

Krupp, H. (1967). Particle adhesion, theory and experiment. Retrieved from https://scholar.google.ca/scholar?q=particle+adhesion+theory+and+experiment&btnG=&hl=en&as_sdt=0%2C5#0

Lauga, C., Chaouki, J., Klvana, D., & Chavarie, C. (1991). Improvement of the fluidisability of Ni/SiO₂ aerogels by reducing interparticle forces. *Powder Technology*. Retrieved from <http://www.sciencedirect.com/science/article/pii/003259109180208Z>

Leu, L., & Huang, C. (1994). Fluidization of cohesive powders in a sound waves vibrated fluidized bed. *AIChE Symposium Series*. Retrieved from <https://scholar.google.ca/scholar?hl=en&q=fluidization+of+cohesive+powders+in+>

a+sound+waves+vibrated+fluidized+bed&btnG=&as_sdt=1%2C5&as_sdtp=#0

- Li, H., Legros, R., Brereton, C. M. H., Grace, J. R., & Chaouki, J. (1990). Hydrodynamic behaviour of aerogel powders in high-velocity fluidized beds. *Powder Technology*, 60(2), 121–129. [http://doi.org/10.1016/0032-5910\(90\)80137-N](http://doi.org/10.1016/0032-5910(90)80137-N)
- Malvern Instruments. (2012). INFORM WHITE PAPER A Basic Guide to Particle Characterization.
- Marinelli, J., & Carson, J. W. (1992). Solve solids flow problems in bins, hoppers, and feeders. *Chemical Engineering Progress*, 88(5), 22–28. Retrieved from <http://cat.inist.fr/?aModele=afficheN&cpsidt=5272137>
- Molerus, O. (1982). Interpretation of Geldart's type A, B, C and D powders by taking into account interparticle cohesion forces. *Powder Technology*, 33(1), 81–87. [http://doi.org/10.1016/0032-5910\(82\)85041-9](http://doi.org/10.1016/0032-5910(82)85041-9)
- Mori, S. (1990). Vibro-Fluidization of Group-C Particles and its Industrial Application. *AIChE Symp. Ser.*, 86(276), 88–94. Retrieved from <http://ci.nii.ac.jp/naid/10011183507/en/>
- Morooka, S., Kusakabe, K., Kobata, A., & Kato, Y. (1988). Fluidization state of ultrafine powders. *Journal of Chemical Engineering of Japan*, 21(1), 41–46. Retrieved from <http://cat.inist.fr/?aModele=afficheN&cpsidt=7723152>
- Nedderman, R. M. (2005). *Statics and kinematics of granular materials. Annals of Physics* (Vol. 54).
- Pacek, A. W., & Nienow, A. W. (1990). Fluidisation of fine and very dense hardmetal powders. *Powder Technology*, 60(2), 145–158. [http://doi.org/10.1016/0032-5910\(90\)80139-P](http://doi.org/10.1016/0032-5910(90)80139-P)
- Pajonk, G. M. (1991). Aerogel catalysts. *Applied Catalysis*, 72(2), 217–266. [http://doi.org/10.1016/0166-9834\(91\)85054-Y](http://doi.org/10.1016/0166-9834(91)85054-Y)
- Particle Technology and Applications*. (2012). CRC Press. Retrieved from <https://books.google.com/books?id=dznOBQAAQBAJ&pgis=1>
- Peleg, M., & Mannheim, C. H. (1973). Effect of conditioners on the flow properties of powdered sucrose. *Powder Technology*, 7(1), 45–50. [http://doi.org/10.1016/0032-5910\(73\)80007-5](http://doi.org/10.1016/0032-5910(73)80007-5)

- Ren, Z. F., Huang, Z. P., Xu, J. W., Wang, J. H., Bush, P., Siegal, M. P., & Provencio, P. N. (1998). Synthesis of large arrays of well-aligned carbon nanotubes on glass. *Science*, 282(5391), 1105–1107. <http://doi.org/10.1126/science.282.5391.1105>
- Schubert, H. (1984). Capillary forces - modeling and application in particulate technology. *Powder Technology*, 37(1), 105–116. [http://doi.org/10.1016/0032-5910\(84\)80010-8](http://doi.org/10.1016/0032-5910(84)80010-8)
- Seville, J. P. K., Willett, C. D., & Knight, P. C. (2000). Interparticle forces in fluidisation: a review. *Powder Technology*, 113(3), 261–268. [http://doi.org/10.1016/S0032-5910\(00\)00309-0](http://doi.org/10.1016/S0032-5910(00)00309-0)
- Visser, J. (1989a). Van der Waals and other cohesive forces affecting powder fluidization. *Powder Technology*, 58(1), 1–10. [http://doi.org/10.1016/0032-5910\(89\)80001-4](http://doi.org/10.1016/0032-5910(89)80001-4)
- Visser, J. (1989b). Van der Waals and other cohesive forces affecting powder fluidization. *Powder Technology*, 58(1), 1–10. [http://doi.org/10.1016/0032-5910\(89\)80001-4](http://doi.org/10.1016/0032-5910(89)80001-4)
- Wang, Z., Kwauk, M., & Li, H. (1998). Fluidization of fine particles. *Chemical Engineering Science*, 53(3), 377–395. [http://doi.org/10.1016/S0009-2509\(97\)00280-7](http://doi.org/10.1016/S0009-2509(97)00280-7)
- Xie, H. Y. (1997). The role of interparticle forces in the fluidization of fine particles. *Powder Technology*, 94(2), 99–108. [http://doi.org/10.1016/S0032-5910\(97\)03270-1](http://doi.org/10.1016/S0032-5910(97)03270-1)
- Yan, H., & Barbosa-Canovas, G. V. (1997). Compression characteristics of agglomerated food powders: Effect of agglomerate size and water activity Caracteristicas de la compresion de alimentos en polvo: Efecto del tamano del aglomerado y del contenido de humedad. *Food Science and Technology International*, 3(5), 351–359. <http://doi.org/10.1177/108201329700300506>
- Zhou, T., & Li, H. (1999). Effects of adding different size particles on fluidization of cohesive particles. *Powder Technology*. Retrieved from <http://www.sciencedirect.com/science/article/pii/S0032591098002113>
- Zhu, J; Zhang, H. (2004, December 21). Fluidization additives to fine powders. U.S. Patent Application 6833185, January 15, 2004. Retrieved from <https://www.google.com/patents/US6833185>

Chapter 3

Flow Properties of Fine Powders

Within many industries, powders are used in a broad range of processes and it is often essential to understand how a powder will behave in order to properly design the process and equipment. Powder flowability is related to many process such as flow from storage silos, undergo fluidization, or pneumatic transportation, blending, screening, grinding, granulation and tableting, etc. Flow behavior is multidimensional and does in fact depend on many powder characteristics. For this reason, no one test could ever quantify flowability (Prescott & Barnum, 2000). To predict how a powder will perform in any of these processes, a diverse array of different characterization techniques have been developed which can be used to test powders under widely varying conditions.

The most well-known powder characterization technique is probably the measurement of shear strengths under different normal stresses using a Jenike shear cell. Plotting these shear strengths against the normal stresses constructs a yield locus, from which several parameters can be generated such as angle of internal friction, cohesion, major principal stress at a critical state and unconfined yield strength. The ratio of major principal stress to unconfined yield strength was employed by Jenike to categorize powders into five groups ranging from non-flowing to free flowing (Carr, 1965; Jenike, 1964). Following the same principle, different types of shear cells have been developed, such as an annular shear cell, a Schulze ring shear tester and a shear cell modules of FT4 Powder Rheometer. On another route, Carr⁶ proposed a series of indices that combine the results from multiple characterization techniques (angle of repose, compressibility, angle of spatula and angle of fall, uniformity and Carr's cohesion) into a single flowability score to classify powders into 7 groups with flowability ranging from very poor to very good.

Currently people in powder handling and processing field believed that powder characterization techniques should match the powder application and the process equipment to be used (Ploof & Carson, 1994; Jörg Schwedes, 2003). Krantz et al further classified powder flow characterizing techniques into three groups including dynamic, dynamic-static and static according to the state of a powder sample when the characterization is carried out (Krantz, Zhang, & Zhu, 2009). They suggested that flow property results characterized under different states are not interchangeable. To fully understand the powder flow behaviors, the flow properties have to be characterized using the techniques in this study.

3.1 Experimental Particles and Preparation

In this study, powder samples were prepared by blending the virgin powder and the additives. Generally, many methods can be used for surface coating of cohesive particles with finer particles as flow conditioners, such as high-shear mixing and sieving. In order to ensure the particle size unchanged, the sieving method was used in this study (high-shear mixing would normally reduce the particle size). As shown in Figure 3.1, the powder samples were sieved twice by ultrasonic vibrating screen (325 mesh). More detailed discussion can be found in a published patent (Zhu, J; Zhang, 2006). 7 host particles are contained: 4 fine particles including glass beads (6 and 10 μm), talcum powder 18.5 μm and polyurethane 22 μm ; and 3 coarser particles including glass beads (39, 65 and 138 μm) used for comparative studies in the experiments. The key properties of these host particles are given in Table 3.1. Nanoparticles of SiO_2 with a spherical shape and a mean diameter of 16 nm is used as guest particles, and the mass percentage of guest particles in the percentage of host particles varies from 0 up to 1.5%.

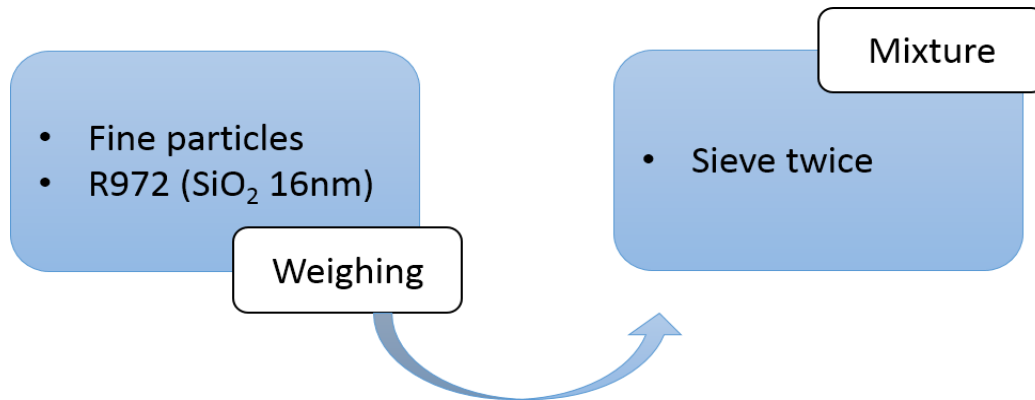


Figure 3.1 Flow chart for preparation of powder samples

Scanning electron microscopy (S-2600N Scanning Electron Microscope, Hitachi Ltd., JP) is applied to study the surface morphology and surface quality of the resulting particles after mixing. The flowability of the coated particles is characterized through measuring the cohesion test, angle of repose (AOR), avalanche angle (AVA), and through the conventional fluidization tests.

Table 3.1 Physical properties of the experimental powders

Powder Name	Particle Size (μm)	Material	Shape	Particle Density (kg/m^3)	Bulk Density (kg/m^3)	Geldart Powder Classification
Glass beads	6	Soda-lime-Silica glass	Spherical	2500	704	C
Glass beads	10	Soda-lime-Silica glass hydrous	Spherical	2500	738	C
Talc	18	magnesium silicate	Irregular	2750	713	C
PU	22	Polyurethane	Irregular	1200	689	C
Glass beads	39	Soda-lime-Silica glass	Spherical	2500	1301	A
Glass beads	65	Soda-lime-Silica glass	Spherical	2500	1254	A
Glass beads	138	Soda-lime-Silica glass	Spherical	2453	1421	A

3.2 Cohesion

The cohesion value were tested by an FT4 Powder Rheometer manufactured by Freeman Technology, representing the static flowability of all samples. In this test, 3 main steps are included in this procedure. A schematic of the FT4 Powder Rheometer shear cell modules is illustrated in Figure 3.2. Foremost, powder sample in a 50 mm diameter cylindrical vessel was conditioned and pre-sheared, to be arranged into a homogenized state by a rotating blade downwards and upwards 4 cycles. Then the vessel was split to level the powder volume at 120 ml (1/2 cup) and the blade would be replaced by a vented piston that allows air to escape away from the powder. Following a standard process established by Jenike (ASTM D6128 - 06 Standard Test Method for Shear Testing of Bulk Solids Using the Jenike Shear Cell, 2006; Kamath, Puri, Manbeck, & Hogg, 1993; J. Schwedes & Schulze, 1990), the powder were compressed under a specified normal stress of 9 KPa across the whole cross-section of the test cup. Afterwards, the vented piston was exchanged for a shearing tool and the sample was slowly rotating sheared under the same specified normal stress until a constant shear stress was reached. This is referred to as pre-shearing and was used to place the powder in a critical state, which was incorporated to increase repeatability between tests. Once in this critical state, the powder sample was placed under a normal stress that was lower than the normal stress used for pre-shearing and sheared again. The shear stress measured in this step was then used to define a point on the yield locus of the compressed powder. After that, a repeated pre-shearing procedure started and shear stress at lower normal stress was also measured, to obtain additional points on the yield locus. The yield shear strengths were measured at normal stresses of 7, 6, 5, 4 and 3 KPa respectively. Finally the cohesion value was obtained by extrapolating the yield locus to zero normal stress. For each sample, 2-3 measurements were repeated and the average was used to construct the yield locus to ensure accuracy.

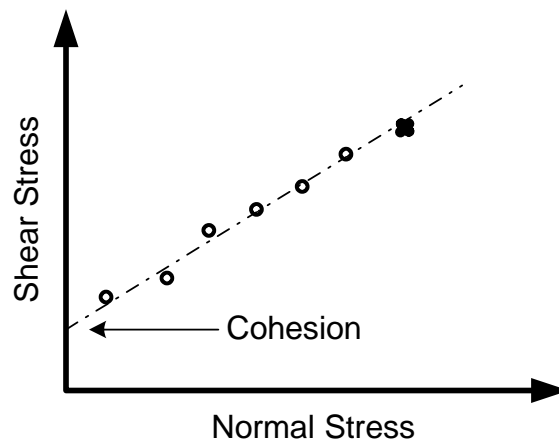
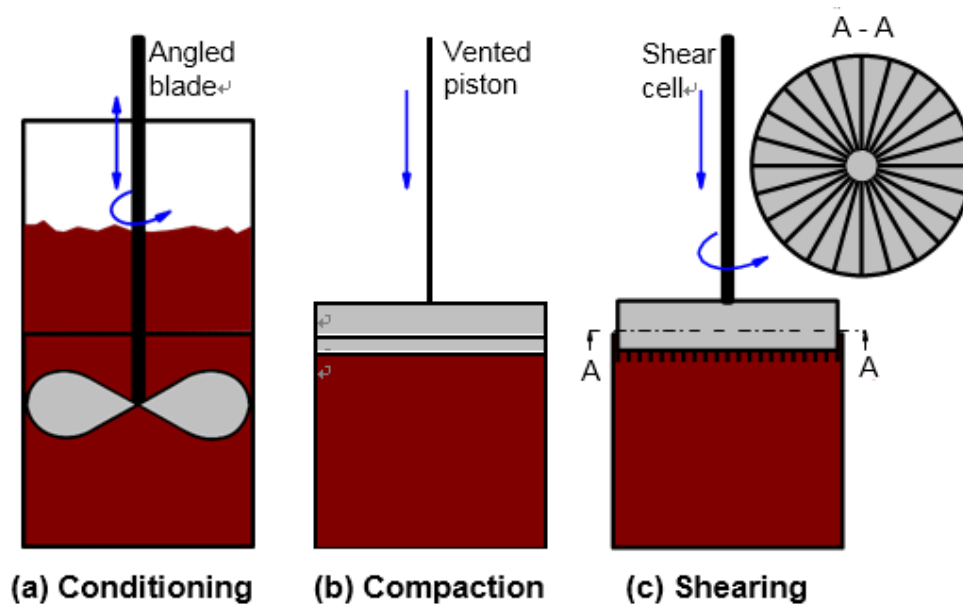


Figure 3.2 Schematic diagram of shearing strength measurement using a FT4 Powder Rheometer

The figure 3.3 shows the cohesion value of the glass beads powder samples blended with 16 nm SiO₂ (R972), respect to the concentration of nanoparticles. For Glass beads 10 μm which is a typical Geldart group C particle (Geldart, 1973), with the increasing concentration of nanoparticles, the cohesion value expresses a general declining trend reflecting the improvement of the powder's flow properties by nanoparticles. While, the concentration of nanoparticles at 1.5%w/w increased again which indicates that the additive concentration exists a minimum at around 1%w/w, shown in Figure 3.6. Figure

3.4 (A) and (B) conveys an obvious phenomenon that as the particle size goes up, particle cohesion value is reduced. As mentioned in Chapter 2, interparticle forces are an important factor for group C particles, when the particle size grow up to Geldart group A the cohesion value decrease obviously. Although additive do improve the powder flowability, the cohesive properties cannot be eliminated, but just reduced to some extent. It also noticed that, for Geldart group A particles like glass beads 39 even larger, the additive influence almost inconspicuous. But for cohesive particles, the additive effect is truly significant.

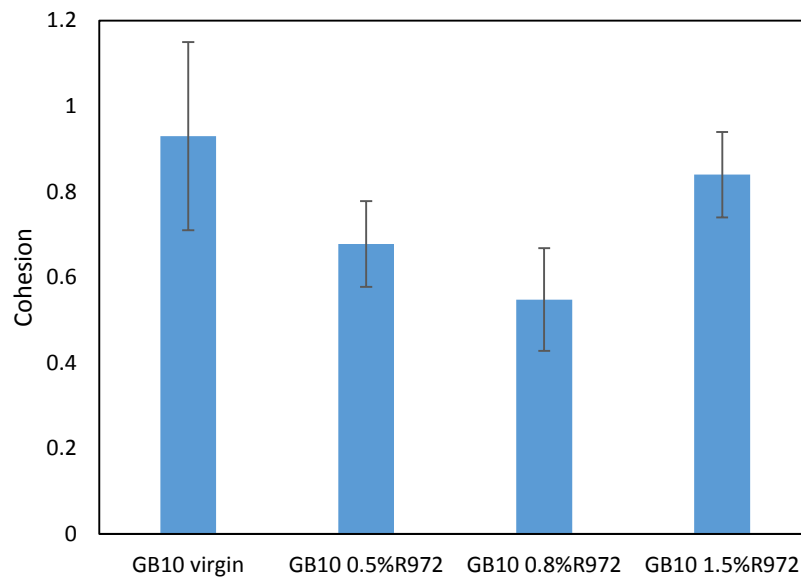


Figure3.3 Cohesion of glass beads 10 μm blended with nanoparticles

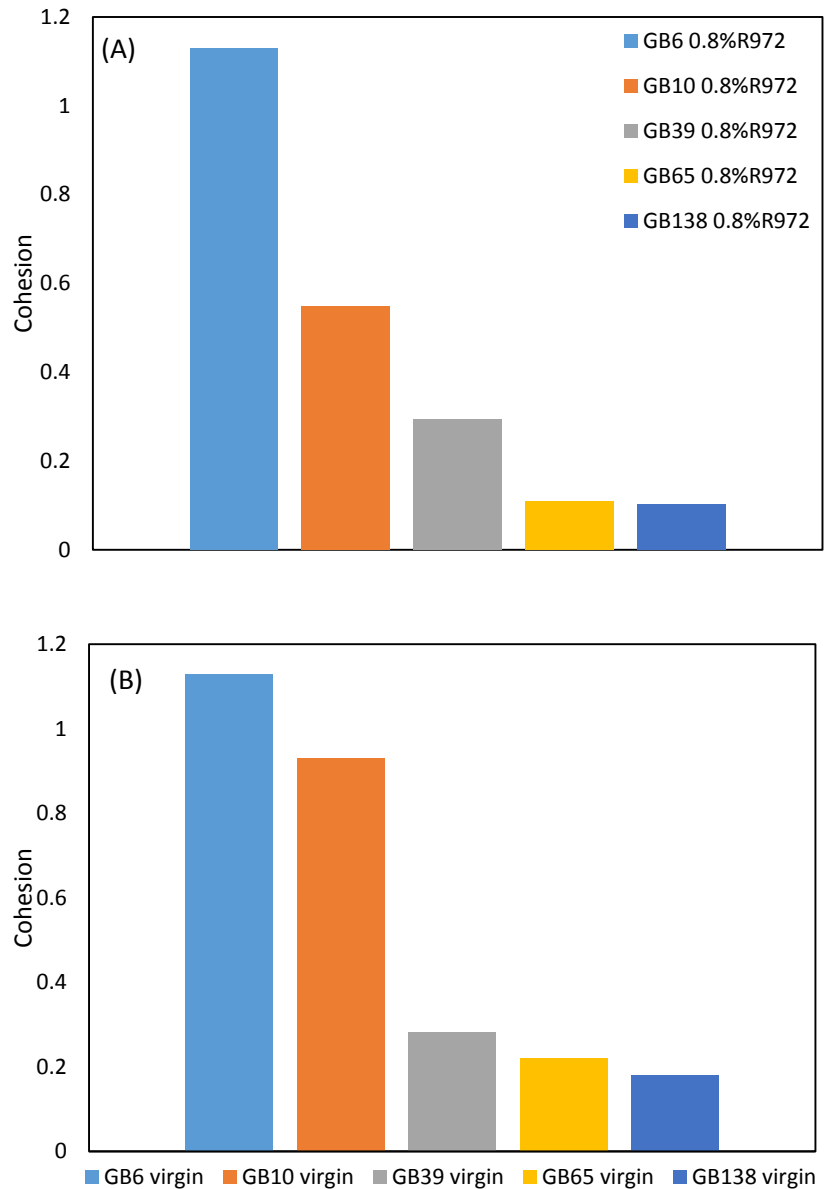


Figure 3.4 Cohesion of different particle size
 (A) Glass beads blended with 16 nm SiO₂ (B) Glass beads virgin particles

3.3 Angle of Repose

Angle of repose (AOR) is the largest angle at which powders can pile up, considered as a semi-static flowability parameter. Generally, it is related to the powders' cohesiveness and internal friction and it is widely used to characterize flow properties of powders.

Measurement of the angle of repose was carried out using a PT-N Hosokawa Powder Characteristic Tester, following the standardized testing procedures of ASTM D6369-08 (Standard Test Method for Bulk Solids Characterization by Carr Indices, 1999).

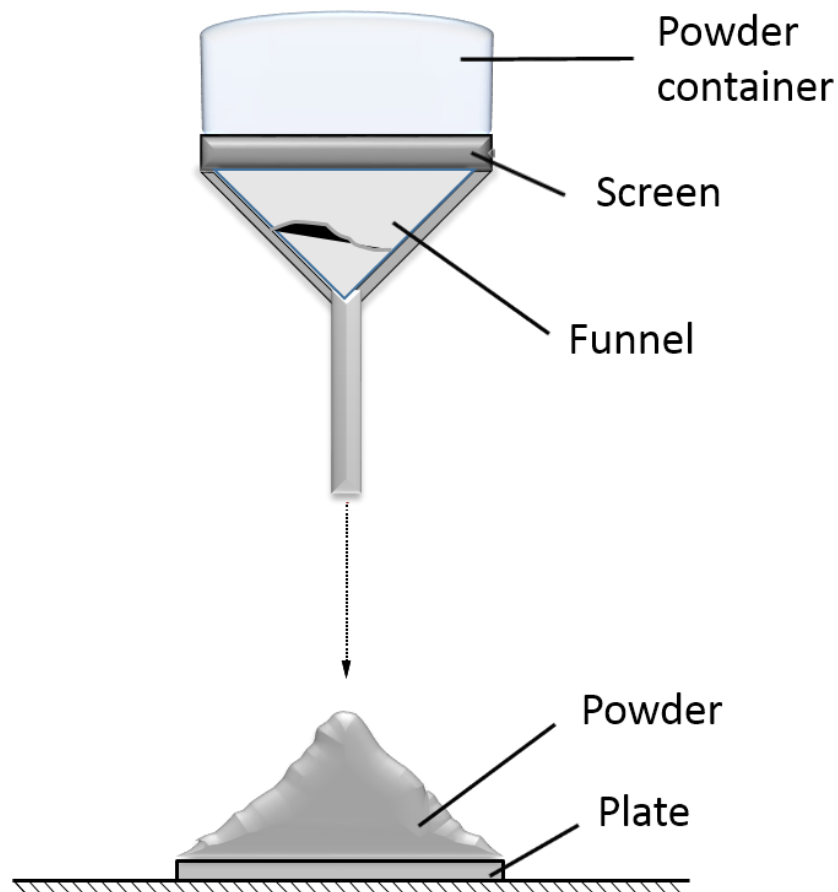


Figure 3.5 Schematic diagram of a Hosokawa powder tester for angle of repose measurement

As shown schematically in Figure 3.5, the AOR was then measured as the angle between the surface of the powder heap and the surface of the plate. For each test, powder samples were loaded on the screen with a vibrator. By adjusting the vibration intensity, the powder was controlled to fall down through the funnel, in a slow and consistent rate. The powder would be delivered onto a circular plate which was aligned under the funnel, and form a conical heap. When the powder heap covered the entire plate surface, also, there was no additional accumulation of powder could be added onto the powder heap,

then the angle of repose could be measured. This procedure was repeated 3-6 times for each powder sample and 3 data with difference smaller than 0.6 were selected. The average of the 3 data values were used as the AOR.

Generally, smaller value of AOR indicates the better flowability. The table below is a category of powder classified by angle of repose values (Cheremisinoff & Cheremisinoff, 1984):

Table 3.2 Classification of flow properties by angle of repose

Angle of Repose	Flow properties
$25^\circ < \theta < 30^\circ$	Very free-flowing
$30^\circ < \theta < 38^\circ$	Free-flowing
$38^\circ < \theta < 45^\circ$	Fair to passable flow
$45^\circ < \theta < 55^\circ$	Cohesive
$55^\circ < \theta < 70^\circ$	Very cohesive

Angle of repose as a semi-static flow parameter, reveals similar results with cohesion value. Figure 3.6 clarifies the angle of repose value of glass beads 10 μm blended with respect to nanoparticle concentration. It's also proved that flowability improvement by adding nanoparticles, and after the decreasing value, 1.5%w/w also appears a little increase by testing angle of repose. The different compared with cohesion, is that the value of 0.5%w/w and 0.8%w/w nearly no difference. Two explanation may be possible. First is that the minimum value is between 0.5% and 0.8%w/w nanoparticle concentration, which indicates the cohesion and angle of repose has different optimum. Another guess is that the error always exists although the repeat test make our experiment results accuracy, so the cohesion of 0.5% and 0.8%w/w actually is in partial coincidence, which is also reasonable.

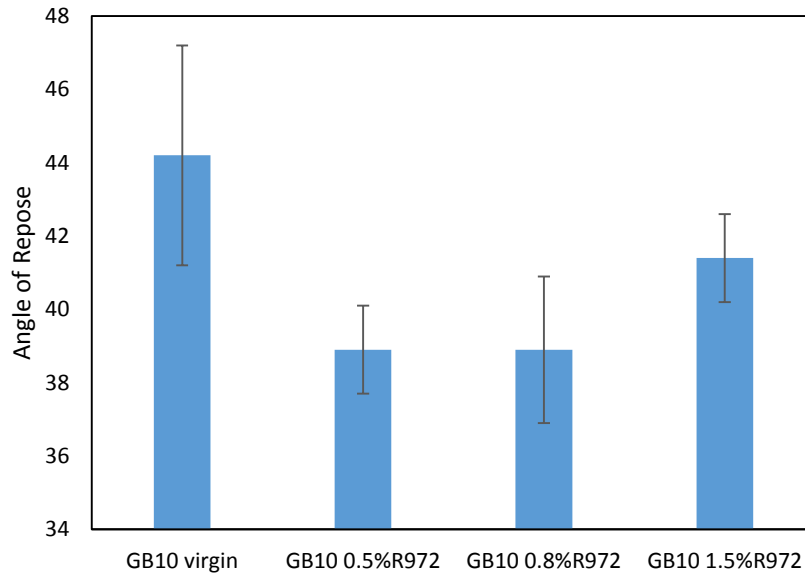


Figure 3.6 Angle of repose of glass beads blended with R972

Figure 3.7 exhibits the angle of repose values of powder samples blended with R972, respect to their particle size. Reference to the classification of flow properties by angle of repose (Cheremisinoff & Cheremisinoff, 1984), particle was free to flow when angle of repose value is below around 40° . The additive advantage of glass beads 6 and 10 μm were more apparent than larger particles, whose virgin particle have already been flowed well. The trend of flowability reflected by angle of repose and cohesion looks similar, but not equal. For glass bead 6 μm blended with SiO_2 , both angle of repose and cohesion still shows a high value, which means the improvement by adding nanoparticles was not always helpful, especially for micron-sized particles. The research on optimum additive concentration for particle size near to 1 μm need further studies.

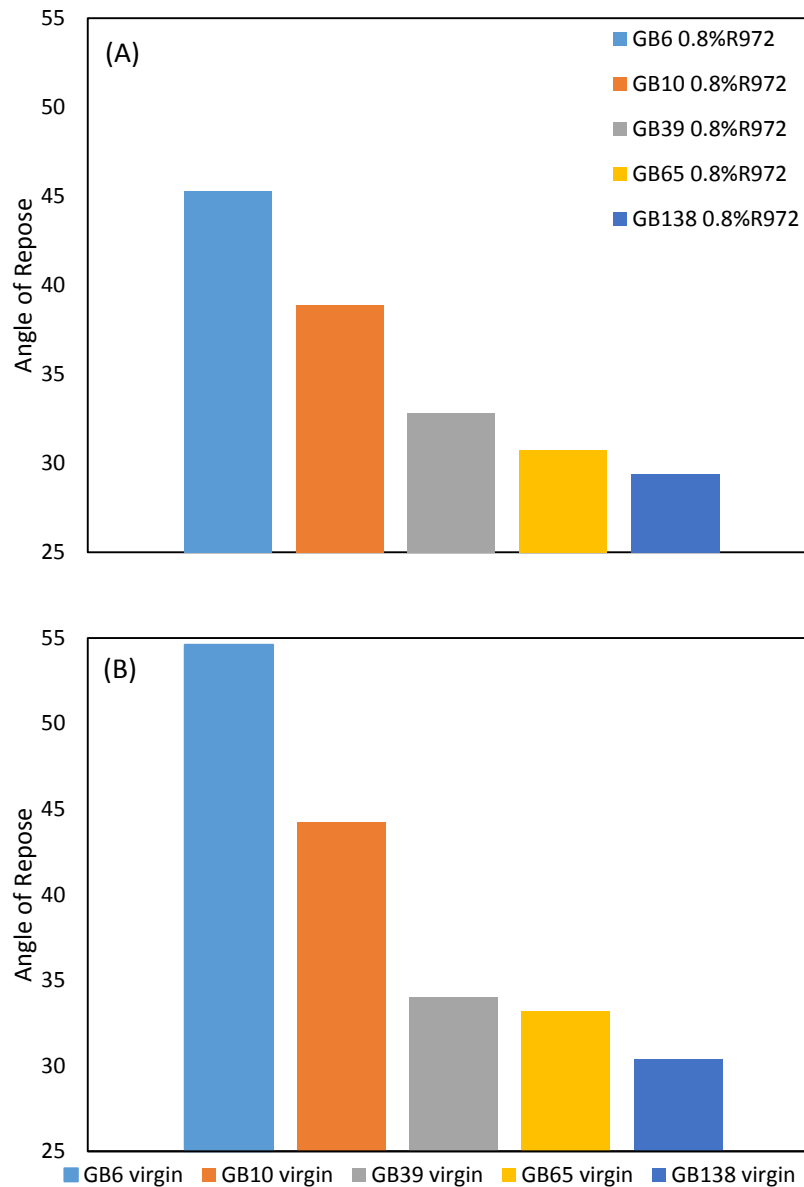


Figure 3.7 Angle of repose of different particle size
 (A) Glass beads blended with 16 nm SiO₂ (B) Glass beads virgin particles

3.4 Avalanche Angle

Avalanche angle (AVA) is refer as the powder flow in a semi-dynamic state, were measured by a powder analyzer (Revolution Powder Analyzer, Mercury Scientific Inc., US). AVA means the maximum angle when powders' avalanche occur at a lower rotating speed. The

schematic diagram of AVA test is shown in Figure 3.8.

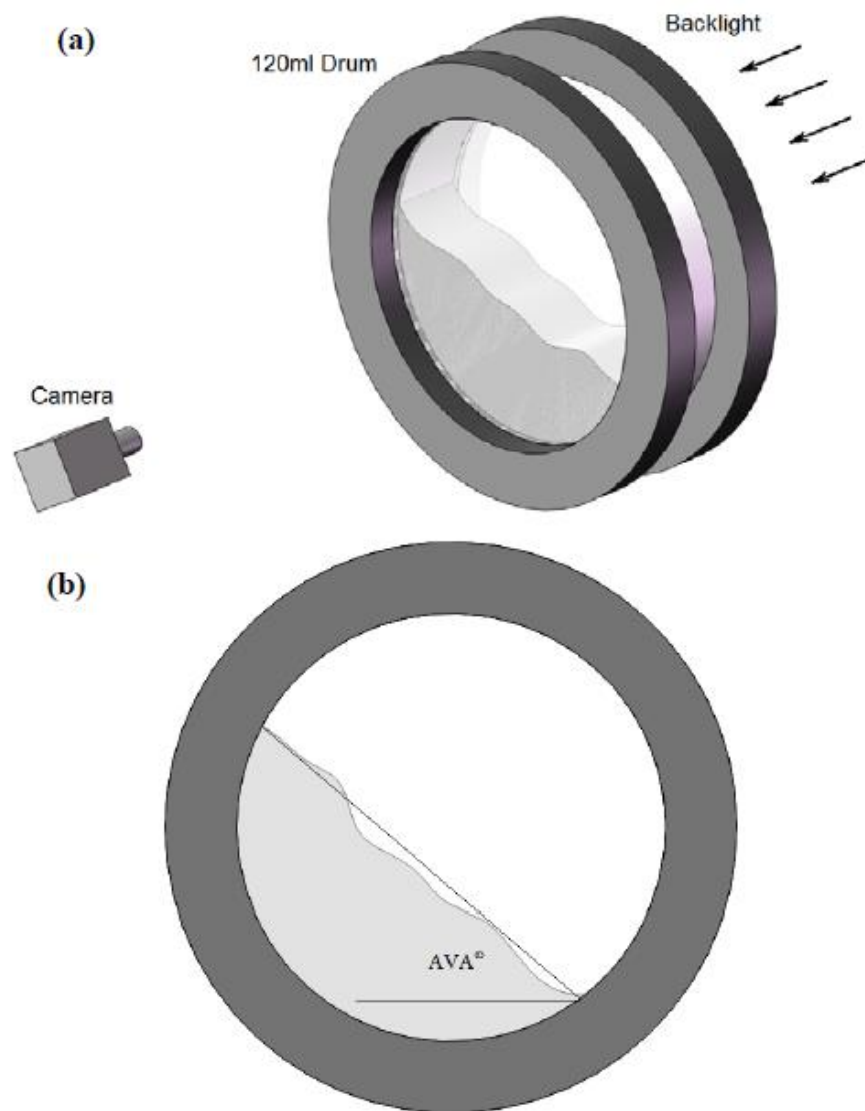


Figure 3.8 Schematic of AVA measurement (a) AVA test system (b) Avalanche Angle

In this test, a tapped volume of 120 mL of powder was weighted by filling a metal cup that was gently tapped 10 times. Any excess powder above the rim of the measuring cup was scraped off using a panel. This process repeat 3 times and then the powder was placed into an 11.0 cm diameter, 3.5 cm wide cylindrical drum with transparent glass sides, a standard accessory of the Revolution Powder Analyzer. The drum was rotated at 0.6 rpm

and a digital camera connected to a computer was used to monitor the flow behavior of the powder. Due to the rotation of the drum, the powder would be carried up the side of the drum until it could no longer support its weight, causing it to collapse or avalanche. In this process, a computer with manufacturer supplied software was used to monitor the angle of the powder surface and record the maximum angle that would occur before an avalanche. The drum was continuously rotated until 200 times avalanches occurred and then the average avalanche angle was provided.

The avalanche angle characterizes the powder in a similar stress state to the AOR, but instead of building the powder heap by dispersing powder on top, the heap is rotated until the powder surface avalanches. Figure 3.9 shows the relationship between avalanche angle and additive concentration. The optimum additive concentration is around 0.5%w/w, respect to avalanche angle results. As a semi-dynamic parameter, both the trend of flowability are settled, but the minimum value were slightly changed by different method.

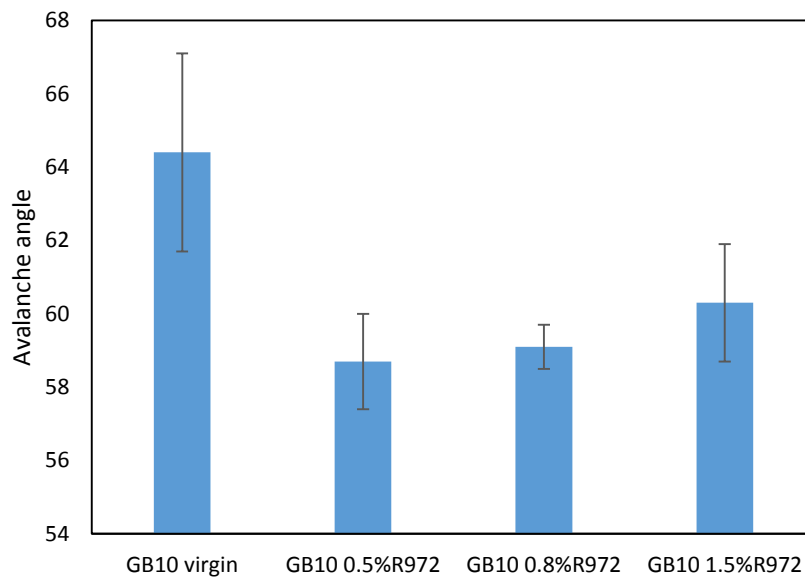
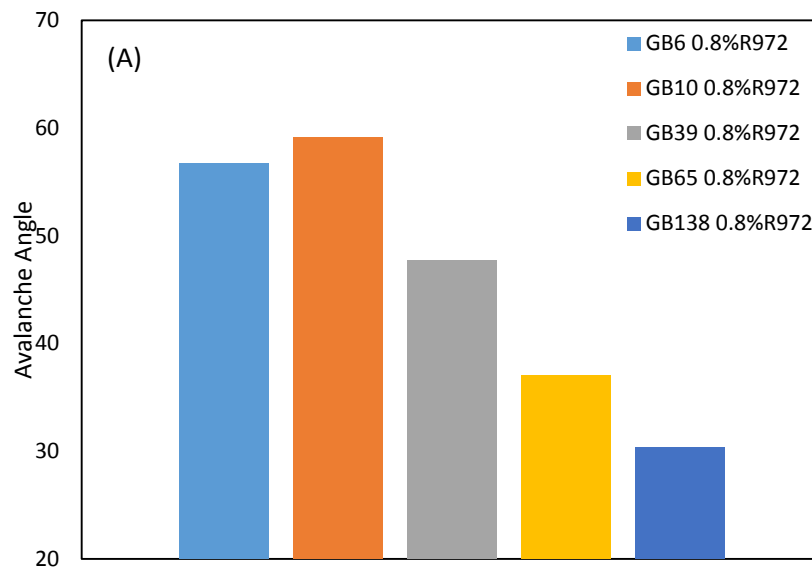


Figure 3.9 Relationship between avalanche angle and additive concentration

From the result in figure 3.10, relationship between avalanche angle and particle size, it looks not sensitive in flowability, compared with cohesion. It was found when particles size are close, like glass beads 6 and 10 μm , the avalanche angle always approach to each other. In this test method, the AVA value always capture by a digital camera, when the cohesive particles cling to the drum, erroneous data occurs. The average error of cohesive powder is about 5.31° and standard deviation is approximately 6.6° , but for Geladart group A particles, the error and standard deviation reduce to 1.51° and 1.94° . But it is expected that the avalanche angle also has improved accuracy because it is fully automated and removes any bias imparted by different operators and the AOR data only records the angle when believing that it is at its maximum.



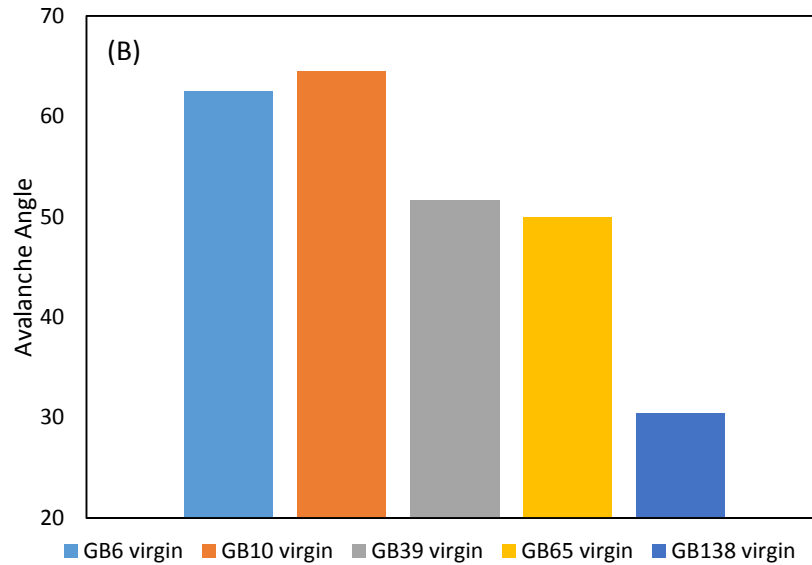


Figure 3.10 Relationship between avalanche angle and particle size (A) Glass beads blended with R972 (B) Glass beads virgin powder

3.5 Comparison of Powder Characterization Techniques

To further investigate the relationship between different characterization techniques, the results obtained from each characterization technique were plotted. Figure 3.11 reveals the relationship between AOR, AVA, Cohesion and BER respect to particle size. Normally, with the particle size increases, flowability increases, so that AOR, AVA and cohesion value should reduce. For smaller particles blended with nanoparticles, these value actually already decreased but still higher than larger particles, the effect of additive can only improve fine particles flowability but not eliminate. So both these four trends were decreasing with particle size increasing.

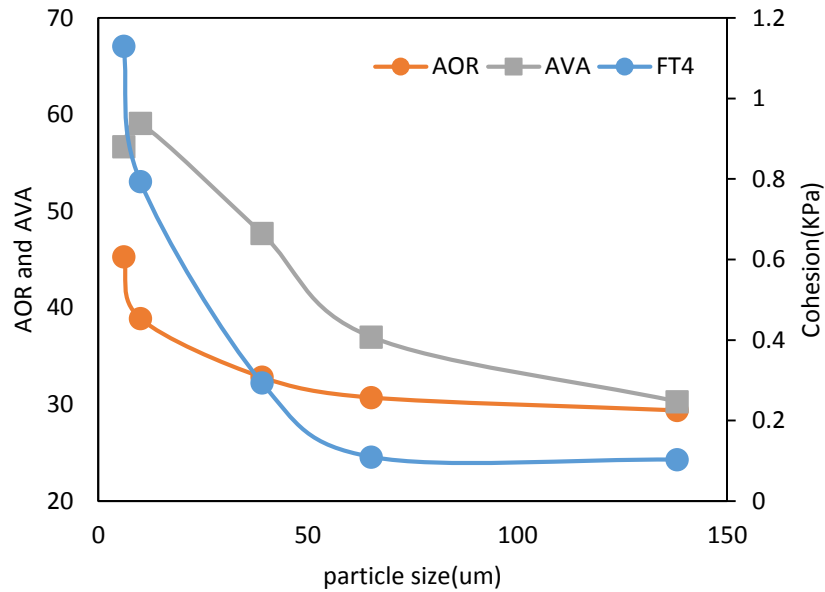


Figure 3.11 Relationship between AOR, AVA, Cohesion and BER respect to particle size (Glass beads blended with nanoparticles)

Figure 3.12 pointed out the relationship between these flow characterization methods respect to additive concentration. As we discussed before, angle of repose, avalanche angle and cohesion value shows slight difference in optimum additive concentration but all around 0.5%-0.8%w/w, so the tendency of these three characterization was a sharp down at beginning and then a little rising, with additive concentration come up. However, when additives were over added, the interparticle force between nanoparticles became dominant, which re-increased their cohesive feature so these value showed a little increasing.

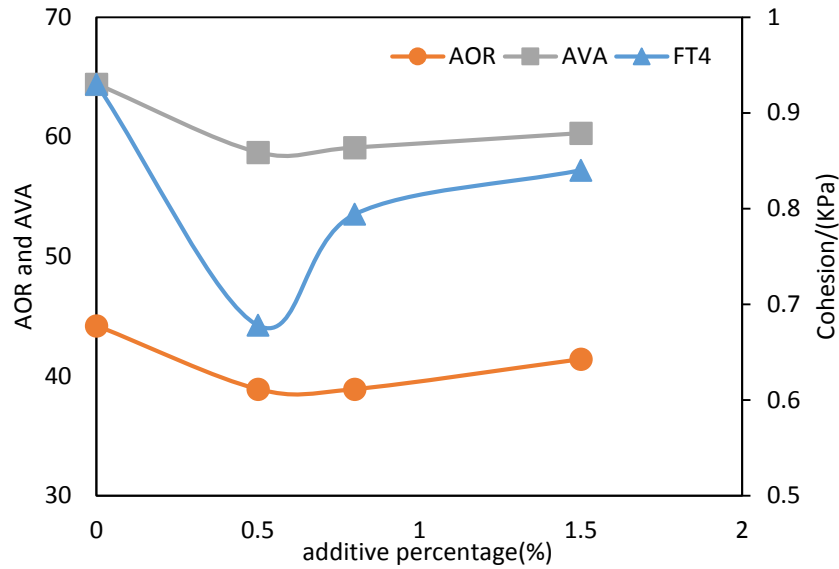


Figure 3.12 Relationship between AOR, AVA and Cohesion respect to additive concentration (glass beads 10 μm)

3.6 Conclusions

Angle of repose, avalanche angle and cohesion were applied to measure the flowability of particles. The measured data often used to design equipment for storage, transportation or general handling of solids. From static to dynamic, flowability were tested with cohesion, AOR and AVA. Powder characterization techniques should match the powder application, and that care must be taken to select the most appropriate characterization technique (Prescott & Barnum, 2000; Jörg Schwedes, 2003). In this study, the flowability of fine particle blended with nanoparticles has been investigated significantly.

Fine particles always present poor flowability, nanoparticles as a flow aid blended into host particle to ensure the improved flow behavior. As shown in AOR, AVA and Cohesion testing method, both exhibits the lower value indicating a better flowability. However, the flowability improvement is in a certain range and can't change powder's inherent

characterization. When the particle size increasing, their angle of repose, avalanche angle and cohesion value still lower than fine particles mixed with nanoparticles.

The results of different characterization methods respect to additive concentration shows the same tendency of reducing firstly then a little going up, but different optimum nanoparticle concentration. Because the measuring method is in static, semi-static, semi-dynamic and dynamic, these techniques should match different powder operating process.

Bibliography

ASTM D6128 - 06 Standard Test Method for Shear Testing of Bulk Solids Using the Jenike Shear Cell. (2006). Retrieved June 4, 2015, from <http://www.astm.org/DATABASE.CART/HISTORICAL/D6128-06.htm>

ASTM D6393 - 08 Standard Test Method for Bulk Solids Characterization by Carr Indices. (1999). Retrieved June 4, 2015, from <http://www.astm.org/DATABASE.CART/HISTORICAL/D6393-08.htm>

Carr, J. (1965). Classifying flow properties of solids. *Chemical Engineering*, 72(3), 69–72. Retrieved from https://www.engineeringvillage.com/blog/document.url?mid=c84_1cf782f941d80c1cM6c7919817173212&database=c84

Cheremisinoff, N. P., & Cheremisinoff, P. N. (1984). Hydrodynamics of gas-solids fluidization. Retrieved from <http://www.osti.gov/scitech/biblio/5909695>

Geldart, D. (1973). Types of gas fluidization. *Powder Technology*, 7(5), 285–292. [http://doi.org/10.1016/0032-5910\(73\)80037-3](http://doi.org/10.1016/0032-5910(73)80037-3)

Jenike, A. (1964). Storage and flow of solids, bulletin no. 123. *Bulletin of the University of Utah*. Retrieved from <http://www.citeulike.org/group/13900/article/11883911>

Kamath, S., Puri, V. M., Manbeck, H. B., & Hogg, R. (1993). Flow properties of powders using four testers — measurement, comparison and assessment. *Powder Technology*, 76(3), 277–289. [http://doi.org/10.1016/S0032-5910\(05\)80009-9](http://doi.org/10.1016/S0032-5910(05)80009-9)

Krantz, M., Zhang, H., & Zhu, J. (2009). Characterization of powder flow: Static and dynamic testing. *Powder Technology*, 194(3), 239–245. <http://doi.org/10.1016/j.powtec.2009.05.001>

Ploof, D., & Carson, J. (1994). Quality control tester to measure relative flowability of powders. *Bulk Solids Handling*. Retrieved from https://scholar.google.com/scholar?q=quality+control+testerto+measure+relative+flowability+of+powders&btnG=&hl=en&as_sdt=0%2C5#0

Prescott, J., & Barnum, R. (2000). On powder flowability. *Pharmaceutical Technology*, 24(October), 60–84. Retrieved from [citeulike-article-id:11996698\http://cat.inist.fr/?aModele=afficheN&cpsidt=795318](http://cat.inist.fr/?aModele=afficheN&cpsidt=795318)

Schwedes, J. (2003). Review on testers for measuring flow properties of bulk solids. *Granular Matter*, 5(1), 1–43. <http://doi.org/10.1007/s10035-002-0124-4>

Schwedes, J., & Schulze, D. (1990). Measurement of flow properties of bulk solids. *Powder Technology*, 61(1), 59–68. [http://doi.org/10.1016/0032-5910\(90\)80066-8](http://doi.org/10.1016/0032-5910(90)80066-8)

Zhu, J; Zhang, H. (2006, February 1). Method and apparatus for uniformly dispersing additive particles in fine powders. Retrieved from <https://www.google.com/patents/US7878430>

Chapter 4

Experimental Methods and Preliminary Study on Fine Particle Fluidization with Nano-Additives

4.1 Experimental Apparatus

The apparatus used for the fluidization experiments is schematically illustrated in Figure 4.1. This fluidization system involved a gas supply and a gas flow control system, a fluidized bed and a U-shape pressure recorder. The compressed air flow through PVC tubing into the bottom of the fluidized bed at both side, and passes through the distributor placed between the fluidized column and the wind box. The wind box was of 5.08 cm I.D. and 12.7 cm in height, above which was a fluidized bed column that was of 5.08 cm I.D. and 45.72 cm in height. Fluidization air contacts with the particles, supports the particle flow, and exits through a bag filter. In each experiments, the fluidized bed was loaded with each powder to an initial height of 13.5 cm. The flow rate control by a digital mass flow controller (Fathom Technologies), which is carefully calibrated before using. Pressure drops across the whole bed are measured by a slant U-shape with an angle of 30°, and bed height could be observed in fluidized column with a scale.

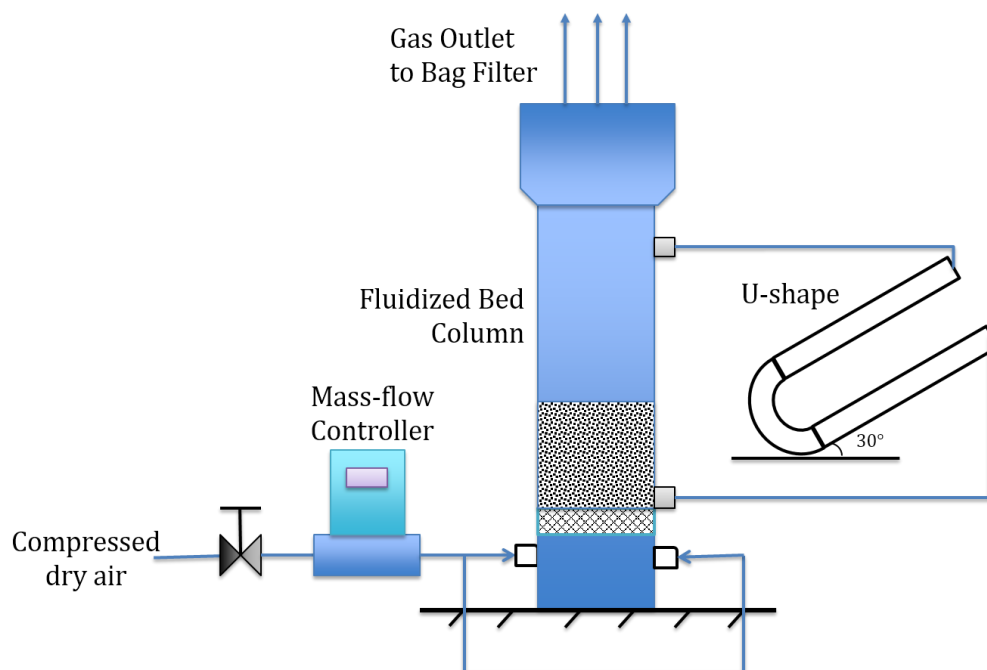


Figure 4.1 Schematic diagram of the fluidized bed system

Fine particle was mixed with nanoparticles by an ultrasonic vibrating method. All details are included in chapter 3.1 and the patent (Zhu, J; Zhang, 2006). Scanning electron microscopy (S-2600N Scanning Electron Microscope, Hitachi Ltd., JP) is applied to study the surface morphology and surface quality of the resulting particles after mixing. In this experiment, the fine particle properties are given in Table 4.1.

Table 4.1 Physical properties of the experimental particles

Powder Name	Particle Size (μm)	Material	Shape	Particle Density (kg/m^3)	Bulk Density (kg/m^3)	Geldart Powder Classification
Glass beads	6	Soda-lime-Silica glass	Spherical	2500	704	C
Glass beads	10	Soda-lime-Silica glass	Spherical	2500	738	C
PU	22	Polyurethane	Irregular	1200	689	C
Glass beads	39	Soda-lime-Silica glass	Spherical	2500	1301	A

Glass beads	65	Soda-lime-Silica glass	Spherical	2500	1254	A
-------------	----	------------------------	-----------	------	------	---

Pressure drop and bed expansion are two main parameters for characterizing the hydrodynamic behaviors of the fluidization.

4.2 Experimental Methodology

4.2.1 Pressure Drops and Minimum Fluidization

In this experiment, the pressure drop are tested by a slant U shape with an angle of 30°. When the gas velocity is low, powder bed stays as a fixed bed and the pressure drop (ΔP) through the bed increases with respect to superficial gas velocity (U) as depicted by the Ergun's equation (Ergun & Orning, 1949) :

$$\frac{\Delta P}{H} = 150 \frac{(1-\varepsilon)^2 \mu_g U}{\varepsilon^3 \bar{d}_{vs}} + 1.75 \frac{(1-\varepsilon) \rho_g U^2}{\varepsilon^3 \bar{d}_{vs}} \quad (4.1)$$

where μ_g and ρ_g are the gas viscosity and density respectively, \bar{d}_{vs} is the equivalent volume-surface mean diameter and ε is the powder bed voidage. The relationship between pressure drop and gas velocity is almost linear. As gas velocity U further increases, when U is up to a critical value, the gravitational force of the powder is balanced by the aerodynamic force exerted by the up-flowing gas. Beyond this time pressure drop and superficial gas velocity no longer obey Ergun equation. After the ΔP up to a maximum, then a little decrease occurs and finally stay at a fixed value, which is the bed static pressure. The final pressure drop through the whole bed equals the powder weight per cross-sectional area of the fluidized bed. Then the drag exerted on the particles equals the net gravitational force exerted on the particles, that is,

$$\Delta P = (\rho_p - \rho_g)(1 - \varepsilon)h \quad (4.2)$$

The critical value of gas velocity defined as minimal fluidization velocity (U_{mf}), separate

fixed bed to fluidized bed. If U reduce slowly to fixed bed, then ΔP will return following a slightly lower route, as shown in Figure 4.2.

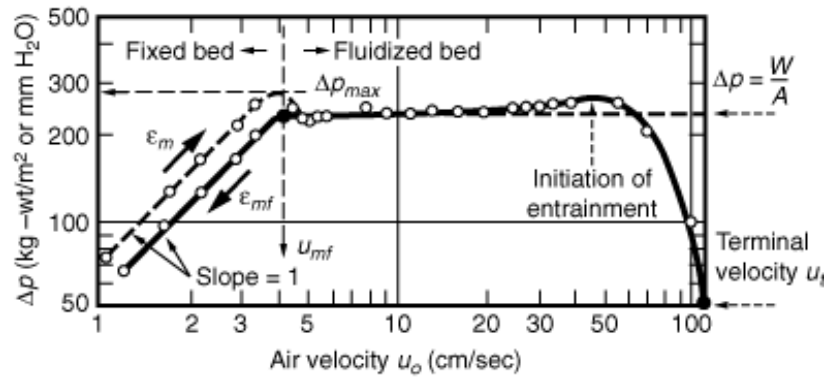


Figure 4.2 Diagram of pressure drop in fluidized bed (Kunii & Levenspiel, 2013)

U_{mf} could be obtained by pressure drop profile tested with decreasing flowrate, the intersection of fixed bed and fluidized bed curve corresponds to minimum fluidization. As increasing flowrate test method experiences hysteresis phenomenon, results are somewhat arbitrary.

In this study, the normalized pressure drop ($\Delta P/m_s g/S$) is adopted, which is defined as the ratio of the measured pressure drops across the whole bed (ΔP) to the net pressure caused by particle weight i.e., $m_s g/S$, where m_s denotes the weight of solids in the bed and S is the cross-sectional area of the fluidized bed. When the entire bed is fluidized, the normalized pressure drop will attain unity and remain stable thereafter even if the gas velocity further increases.

4.2.2 Bed Expansion Ratio

Bed expansion ratio was employed to characterize fluidization quality based on the belief that higher bed expansion indicates more gas in the interstitial void between particles,

implying more uniform gas-solid contact and thereby better fluidization quality. For Geldart groups A particles, their bed expansion ratios are generally less than 1.2; for Geldart groups C powders, due to their cohesive nature leading to poor fluidization, normally with channeling, agglomeration and segregation, it's hard to see bed expansion of cohesive particles. However, When Geldart group C particles could be fluidized, their bed expansion could reach around 2-3 times, much higher than Geldart group A particles although they presented better fluidization properties. Consequently, it seems too arbitrary to correlate the bed expansion ratio and fluidization properties without eliminating the effects from material and other physical properties.

4.3 Difference on Fine Particle Fluidization with or without Nano-additives

As the poor fluidization quality of fine particles, classified in Geldart group C, nanoparticles as a flow aid to improve these cohesive particle fluidization. The mechanism of nanoparticles and mixing method have already included in chapter 2 literature review. This study used 3 kinds of particle, trying to find out some notable characterization in fluidization behaviors for fine powders with fluidization aids, in comparison with those without fluidization aids:

- (1) Although the improvement of fluidization by fluidization aids, those typical poor fluidization behaviors, such as channeling, cracks, plugging and unstable partial fluidization, were still happened. Because the improvement of fluidization by nanoparticles depends on many factors including nanoparticle materials and concentration, even the blending method. For fine particle without fluidization aids, particle always fixed at low superficial gas velocity and poor fluidization behavior occurs as gas velocity increase, sometime high gas velocity could carry partial particles flow away, but sometimes non-fluidization keep on no matter how is the gas

velocity. While after their fluidization improvement, fine particles could reach certain smooth fluidization, but, at lower gas velocity fluidization channeling and agglomerates may still happened. This is attributed to their inherent cohesive properties due to the relatively larger interparticle forces.

- (2) Gledart give the powder classification by particle size and density, in terms of their different fluidization behavior. As we mentioned before, the cohesive particle size is lower than 30 μm , in this size range of particles, there is also some difference in fluidization behavior with and without fluidization aids. Glass beads 6 and 10 μm are the particles we chosen in this experiment. Figure 4.4 is the pressure drop and bed expansion profile which is mixed by 0.8%w/w R972, compared to Figure 4.3 from Huang Qing, normalized pressure drop is up to 0.8, a little higher than virgin particle, and bed expansion ratio improved up 2.4, but without fluidization aids, bed expansion only reached 1.4. While, this improvement shows weak at low velocity, pressure drop profile in Figure 4.4 indicate a partial fluidization even nanoparticles were blended.

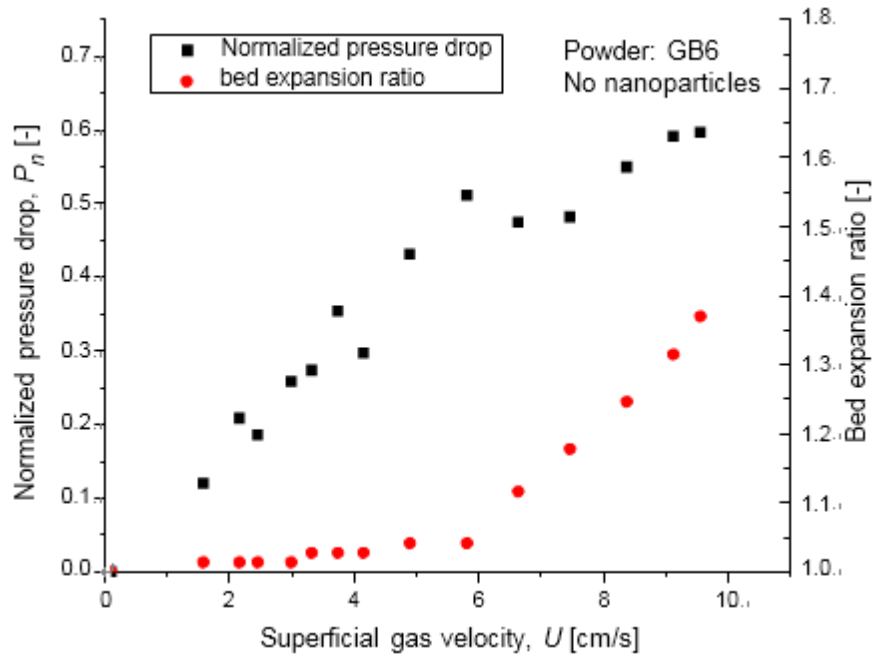


Figure 4.3 Pressure drop and bed expansion of glass beads $6\mu\text{m}$ (Huang, 2009)

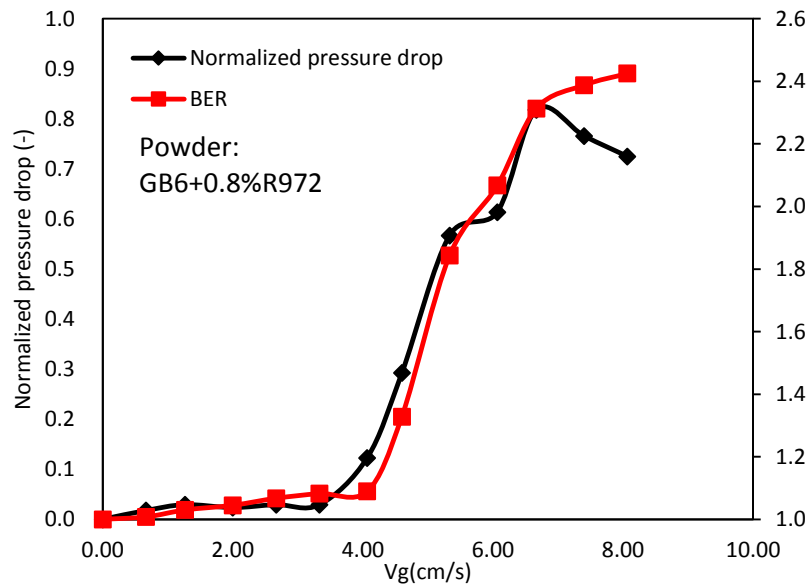


Figure 4.4 Pressure drop and bed expansion of glass beads $6\mu\text{m}$ with 0.8%w/w R972

While for glass beads $10\mu\text{m}$ shown in Figure 4.5, both pressure drop and bed expansion improved quickly with fluidization aid. Glass beads $10\mu\text{m}$ could be fully fluidized and pressure drop value reached 0.9. It's reasonable as the pressure measurement exist error. The lowest pressure test point still have a short distance with distributor, so it's why final

pressure drop couldn't up to 1. For bed expansion, smaller particles have the ability to break big bubbles to keep a smoother suspension in the fluidization bed. In this way, fine particle have the ability to keep micro-voids during fluidization, which guarantee a high bed expansion. However, without nanoparticle covered on host particle surface, the strong interparticle force cause glass beads 10 μm non-fluidzation.

The different appearance of nanoparticle on glass bead 6 and 10 μm may be the particle size distribution and nanoparticle concentration. Although these two particle size is related, the particle size distribution result in different range of smallest and biggest particle size. For glass bead 6 μm particle, the smallest particle size could be sub-micron even nanoparticles, which is related to additive particle size, it's easy to find in Van der Waals force equation that the stronger interaction between two similar particle diameter. For another, both additive concentration of the two glass beads are 0.8%w/w, when particle size reduced, the suitable nanoparticle concentration will be changed, and redundant additive also could form agglomerates and effect particle flowability.

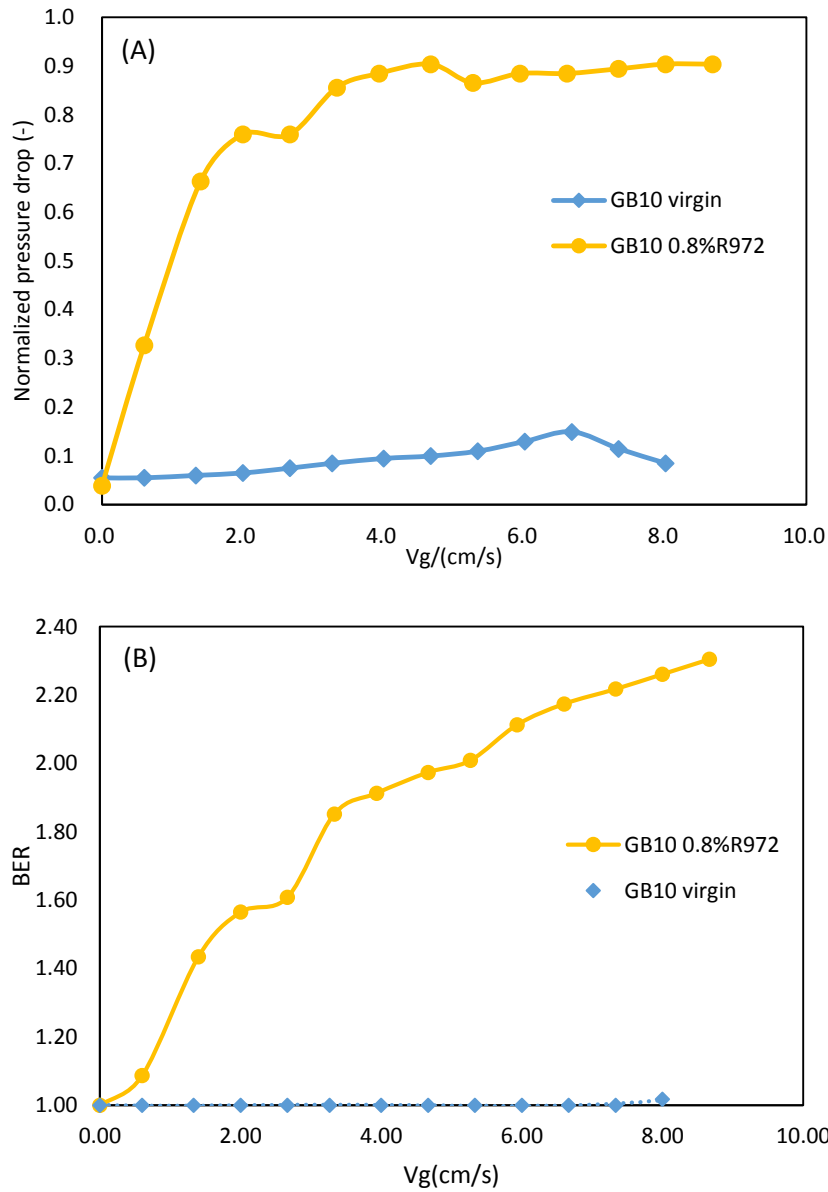
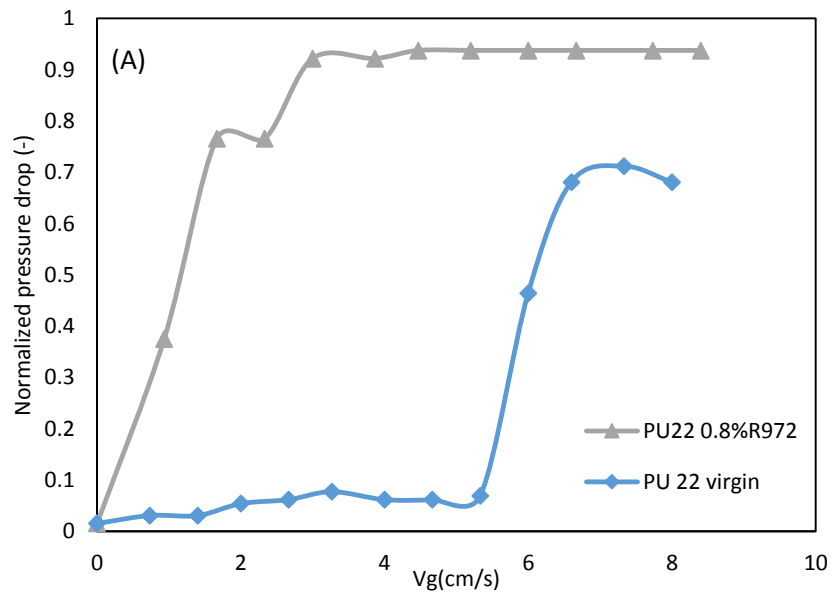


Figure 4.5 Fluidization characterization of glass beads 10 μm
 (A) Normalized pressure drop (B) Bed expansion ratio

(3) Expect to glass beads, this experiment also tried polyurethane 22 μm and Talc 18.5 μm particles. Figure 4.6 showed the difference of PU 22 μm with and without fluidization aid. It's also found the improved fluidization behaviors, a stable pressure drop and higher BER. But for Talc powder, the effect of R972 doesn't show much help compared to virgin powder. These different fluidization of 3 kinds of particles

expressed the practicability and limitation of additives. First of all, nanoparticles do have the ability to improve fluidization of fine particles, but not all types of particles. For glass beads and polyurethane, 16nm SiO₂ is useful as fluidization aid; but for talc powder, when particle size is too small, the task of surface treatment will increase, if surface is rough, which will result in poor performance, and will also affect the processing flow (Xu , Tan Shanxing, 2010). While mechanics of materials could be researched in future study.



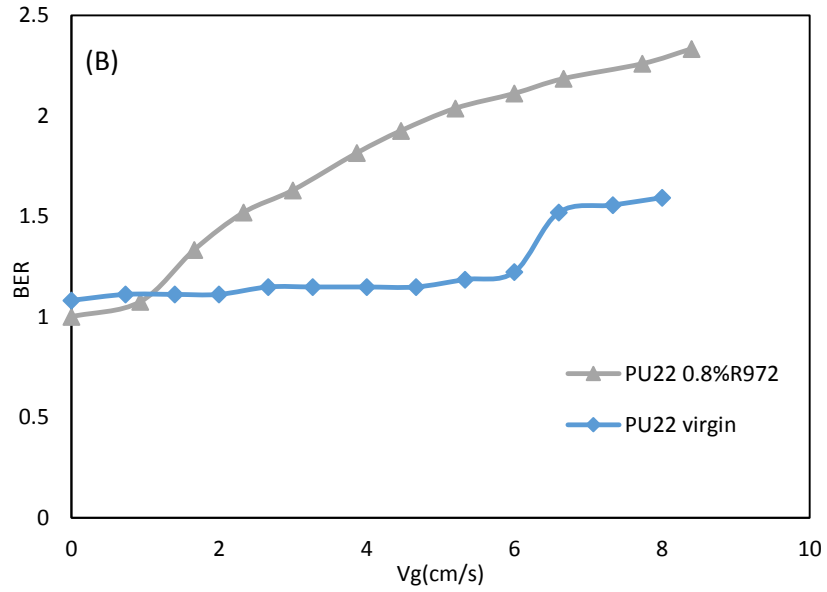


Figure 4.6 Fluidization characterization of polyurethane 21 μm
 (A) Pressure drop (B) Bed expansion ratio

4.4 Discussion on Pressure Drop Test

In particle fluidization, pressure drop often test with decreasing flowrate, because as mentioned before, increasing flowrate test method exists hysteresis phenomenon, results are somewhat arbitrary. However, for fine particles, as the research aim is to character fundamental fluidization behavior with fluidization aids, the experiment of two pressure test method was studied, results were shown in Figure 4.7.

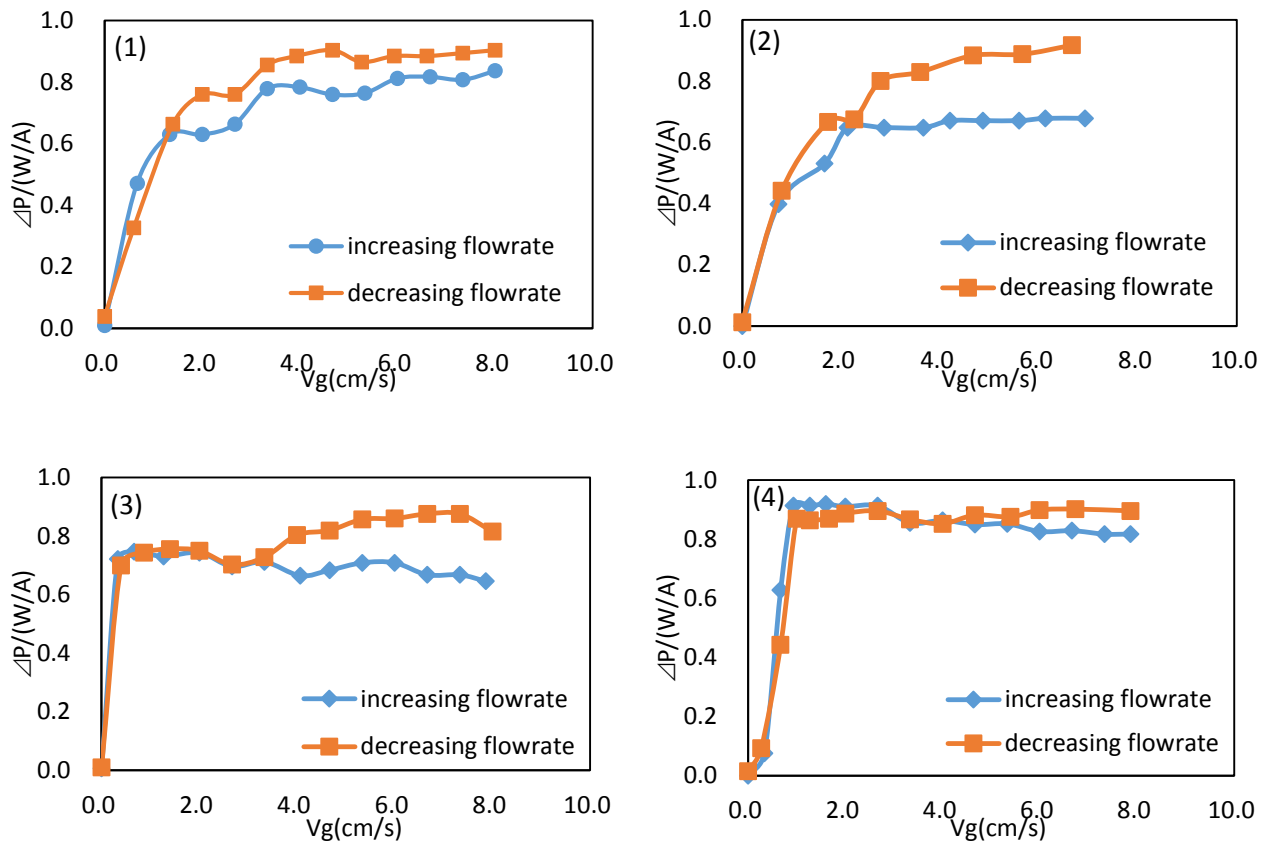


Figure 4.7 Comparison of pressure drop test method
 (1) GB10um 0.8%R972 (2) GB10um 1.5%R972
 (3) GB39um 0.8%R972 (4) GB65um 0.8%R972

After blended with nanoparticles, whether it's Geldart group C or is group A particles, both pressure drop measured by decreasing flowrate is little higher than by increasing flowrate. In decreasing flowrate method, at the beginning gas velocity changed from 0 to 8 cm/s, the a sharp increase give particles a strong drag force, so that more adhered particles break and separately flow. Compared with increasing flowrate method, a higher normalized pressured drop in decreasing flowrate method indicates more particles fluidized in the whole bed. Generally, when particles start to fluidize tested by increasing flowrate method, the first bubble occurred and keep partial pressure inside the bed, at that point pressure drop form a hump in pressure drop curve. For fine particles, it's hard

to form big bubbles even at fluidization beginning, so the uplift in increasing flowrate method haven't been found.

4.5 Effect of Particle Size Distribution

As we all know, the cohesiveness of fine particles make them the difficult to fluidize without any fluidization aids. Channeling and agglomeration as poor fluidization behaviors always occur when gas flow through the fine particle bed. These behaviors were well described and reported in many studies (Geldart, 1973; Valverde & Castellanos, 2007; Wang, Kwauk, & Li, 1998; Zhu, 2003).

However, an interesting phenomenon appears after 2 weeks fluidization test, the pressure drop and bed expansion comes better without any fluidization aids. Figure 4.8 is the pressure drop and bed expansion profile over different stages. At the beginning glass beads 10 μm is non-fluidized and almost no pressure drop exist through the whole bed and the no any expansion during the test time, present as a fixed bed; but after smaller particles blew away, these particles start to fluidize, normalized pressure drop even could be near to 1, and with the superficial gas velocity increases, bed expansion grow to almost 2 times. The improvement doesn't mean their poor fluidization behavior disappeared, but points out the significance of particle size management.

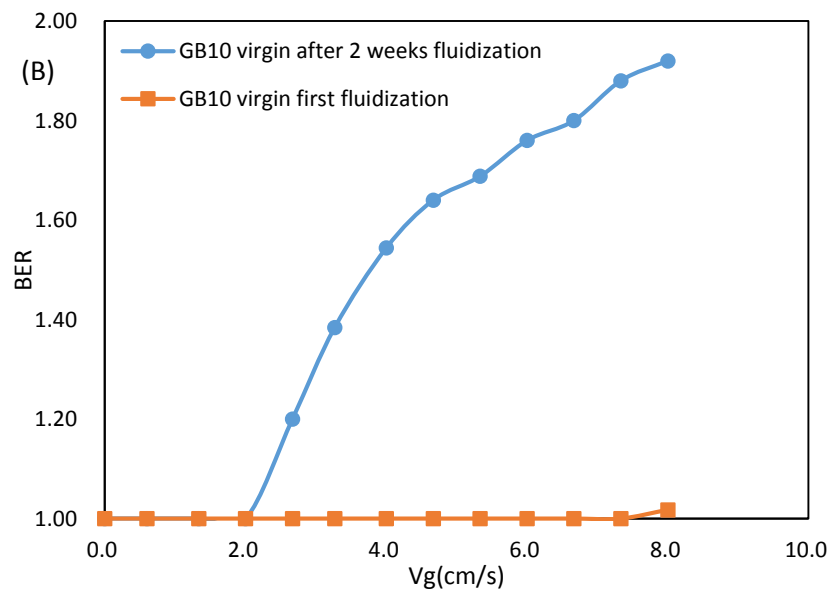
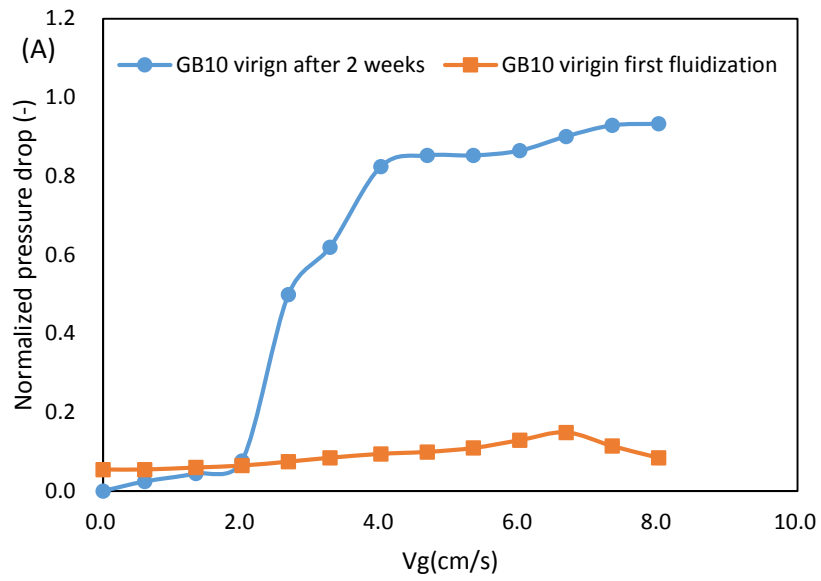


Figure 4.8 Pressure drop and bed expansion profile of glass bead 10 μm virgin particles

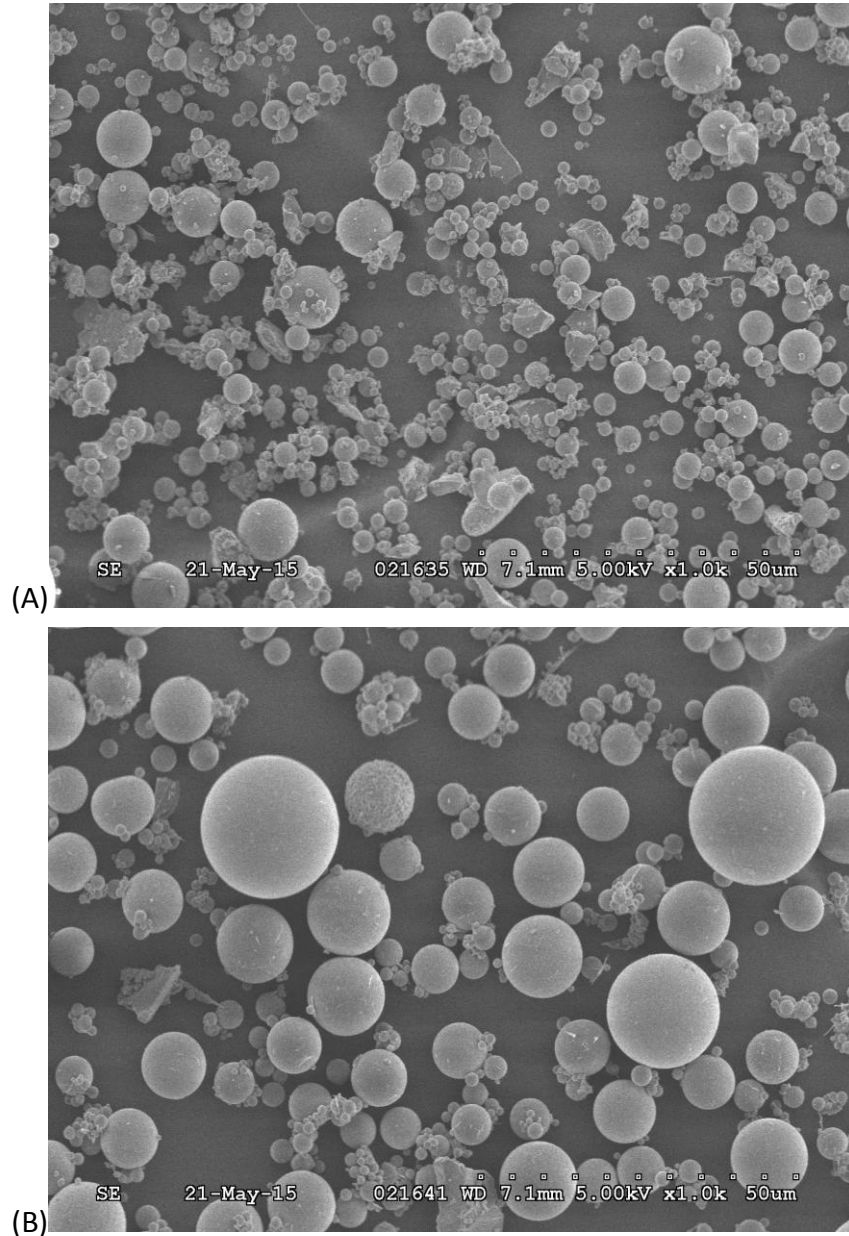


Figure 4.9 SEM of glass beads 10 μm particles
(A) before fluidization (B) after two weeks fluidization

Figure 4.9 shows the particle size difference before and after fluidization. As mentioned in literature review, particle size distribution play a significant role in flowability, also effect particle fluidization quality. In figure 4.4 (A), many finer particles whose size below 10 μm exist, the interparticle forces results in many nature agglomerates. As time goes on, finer particles easily blew away in gas flow, the smaller particles reduced and directly influenced

particle size distribution become narrower and D50 a little increases. Obviously shown in figure 4.4 (B), glass beads exist as single particles, and as the finer particles lose, particle size appears larger than before, because the concentration of larger particles grow up. In this case, particle size distribution as a major factor, significantly affect fine particle fluidization.

For the same major particle size, a narrow particle size distribution indicate a relative minor Van der Waals force. Hamaker has obtain the gravitational energy equation by integration (Wang Hongjun, Li Qihou, Liu Zhihong, Ai Kan, Zhang Duomo, 2006):

$$U_{pp}^0 = -\frac{A}{12Z_0} \frac{d_1 d_2}{d_1 + d_2} \quad (4.3)$$

pp means particles, Z_0 is distance between particles, d_1 and d_2 is the diameter of two different particles, A is Hamaker constant. So the Van der Waals force is:

$$F_{vdw}^0 = -\frac{\partial U_{pp}^0}{\partial Z_0} = -\frac{A}{12Z_0^2} \frac{d_1 d_2}{d_1 + d_2} \quad (4.4)$$

When the diameter of two particles is same, equation becomes as follow:

$$F_{vdw}^0 = -\frac{Ad}{24Z_0^2} \quad (4.5)$$

It's easy to find that Van der Waals force is directly proportional to particle diameter, while particle gravity is proportion to d^3 . When d reduce to a certain value, Van der Waals force would heavier than gravity. For fine particles, Van der Waals force is hundred times bigger than gravity. So when smaller particle were blew away, cohesion created by these particles disappeared and fluidization quality improved. While, as a preliminary study, this phenomenon was found but further studies should be investigated in the future.

4.6 Conclusions

In this chapter, fluidization behaviors of fine particles with and without additives were preliminary studied. Based on the results, the awareness of particle size management,

additive influence to particle size and density, fluidization characterization of fine particle with additives, have some interesting breakthrough.

As fluidization time goes on, fine particles without nanoparticles has an improved fluidization behavior. In fine particle size distribution, smaller particles are easily blow away so that the particle size would be changed, and the escape of finer particles result in a reduced cohesiveness, until a certain point, these particles could be fluidized without fluidization aids.

Nanoparticles as flow conditioner, do have the ability to improve fine particle fluidization quality, but this improvement could not eliminate channeling, agglomerates or other poor fluidization behavior. For particles with different size, optimal additive concentration is changed; for particles with different density, mechanics of materials and their contact force could be researched in future study.

For fine particle with fluidization aids, decreasing flowrate pressure drop test method always could reach a little higher value than increasing flowrate method, indicates more particles fluidized in the whole bed.

Nomenclature

U	Superficial gas velocity, [cm/s]
h	Bed height, [m]
A	Hamaker constant, [-]
ΔP	The whole fluidized bed pressure drop, [KPa]
d_1 and d_2	Diameter of two different particles
Z_0	Distance between particles, [m]
U_{pp}^0	Gravitational energy between two particles, [kJ]
F_{vdw}^0	Van der Waals force
$\Delta P/m_s g / S$	Normalized pressure drop, m_s denotes the weight of solids in the bed, S is the cross-sectional area, [-]
\bar{d}_{vs}	Equivalent volume-surface mean diameter, [cm]

Greek letters

ε	Powder bed voidage, [-]
ρ_p	Particle density, [kg/m ³]
ρ_g	Gas density, [kg/m ³]
μ_g	Gas viscosity, [kg/m/s]

Bibliography

- Ergun, S., & Orning, a. a. (1949). Fluid Flow through Randomly Packed Columns and Fluidized Beds. *Industrial & Engineering Chemistry*, 41(6), 1179–1184.
<http://doi.org/10.1021/ie50474a011>
- Geldart, D. (1973). Types of gas fluidization. *Powder Technology*, 7(5), 285–292.
[http://doi.org/10.1016/0032-5910\(73\)80037-3](http://doi.org/10.1016/0032-5910(73)80037-3)
- Huang, Q. (2009). Flow and fluidization properties of fine powders, *Ph.D.* Retrieved from <http://ezproxy.aut.ac.nz/login?url=http://search.proquest.com/docview/305111253?accountid=8440>
- Krupp, H., & Sperling, G. (1966). Theory of adhesion of small particles. *Journal of Applied Physics*. Retrieved from <http://scitation.aip.org/content/aip/journal/jap/37/11/10.1063/1.1707996>
- Kunii, D., & Levenspiel, O. (2013). *Fluidization Engineering*. Elsevier. Retrieved from <https://books.google.com/books?hl=en&lr=&id=sGkvBQAAQBAJ&pgis=1>
- Valverde, J. M., & Castellanos, A. (2007). Types of gas fluidization of cohesive granular materials. *Physical Review E - Statistical, Nonlinear, and Soft Matter Physics*, 75(3).
<http://doi.org/10.1103/PhysRevE.75.031306>
- Visser, J. (1989). Van der Waals and other cohesive forces affecting powder fluidization. *Powder Technology*, 58(1), 1–10. [http://doi.org/10.1016/0032-5910\(89\)80001-4](http://doi.org/10.1016/0032-5910(89)80001-4)
- Wang Hongjun, Li Qihou, Liu Zhihong, Ai Kan, Zhang Duomo. (2006). Study on Dispersion of Ultra-fine Particle within 2 μ m. *School of Metallurgical Science and Engineering, Central South University*, 1–5.
- Wang, Z., Kwauk, M., & Li, H. (1998). Fluidization of fine particles. *Chemical Engineering Science*, 53(3), 377–395. [http://doi.org/10.1016/S0009-2509\(97\)00280-7](http://doi.org/10.1016/S0009-2509(97)00280-7)
- Xu, Tan Shanxing, H. Y. (2010, August 18). Glass fiber reinforced polycarbonate material and preparation method thereof. Retrieved from <http://www.google.mg/patents/CN101805504A?cl=en>
- Zhou, T., & Li, H. (1999). Effects of adding different size particles on fluidization of cohesive particles. *Powder Technology*. Retrieved from <http://www.sciencedirect.com/science/article/pii/S0032591098002113>

Zhu, J. (2003). Fluidization of fine powders. *Granular Materials: Fundamentals and Applications*, 270–295. <http://doi.org/10.1007/978-94-007-5587-1>

Zhu, J; Zhang, H. (2006, February 1). Method and apparatus for uniformly dispersing additive particles in fine powders. Retrieved from <https://www.google.com/patents/US7878430>

Chapter 5

Effect of Nanoparticles on Gas-Solid Fluidization

For Geldart group C particles with nanoparticles, most researchers focus on their improvement of fluidization quality, but their fluidization characteristics such as pressure drop, minimal fluidization velocity and bed expansion still need more detailed investigation. This chapter gives a comparative study on their fluidization behavior with Geldart group A particles which could be fluidized well and in the range of 25-30 μm to about 150-200 μm .

Bed expansion ratio was employed to characterize fluidization quality based on the belief that higher bed expansion indicates more gas in the interstitial void between particles, implying more uniform gas-solid contact and thereby better fluidization quality. In this experiment, bed expansion were measured in two methods, direct observation and calculation from pressure drop. At higher gas velocity, particle moved fast in fluidized bed and bed height always fluctuated, which increased the difficulty in observing bed height. Each value were tested 3 times and recorded as their average. The ΔP inferred values were also used to describe the variation of the bed height. When particles are fully fluidized, particle moved like fluid ($\Delta P = \rho gh$). Theoretically, the pressure drop of any distance should be proportional. There are 7 measure points on the fluidized bed column, the pressure drop between the lowest two points and the whole bed pressure drop are used to calculate whole bed height. The reason of choosing the two lowest points is that the bed height should always exceed the position of the two points, no matter what is the gas velocity. These two bed height measurement method give both the practical and theoretical value, the comparison are also discussed. Table 5.1 shows the particle properties used in this experiment.

Table 5.1 Physical properties of the experimental particles

Powder Name	Particle Size (μm)	Material	Shape	Particle Density (kg/m^3)	Bulk Density (kg/m^3)	Geldart Powder Classification
Glass beads	10	Soda-lime-Silica glass	Spherical	2500	738	C
PU	22	Polyurethane	Irregular	1200	689	C
Glass beads	39	Soda-lime-Silica glass	Spherical	2500	1301	A
Glass beads	65	Soda-lime-Silica glass	Spherical	2500	1254	A
Glass beads	138	Soda-lime-Silica glass	Spherical	2452.6	1421	A

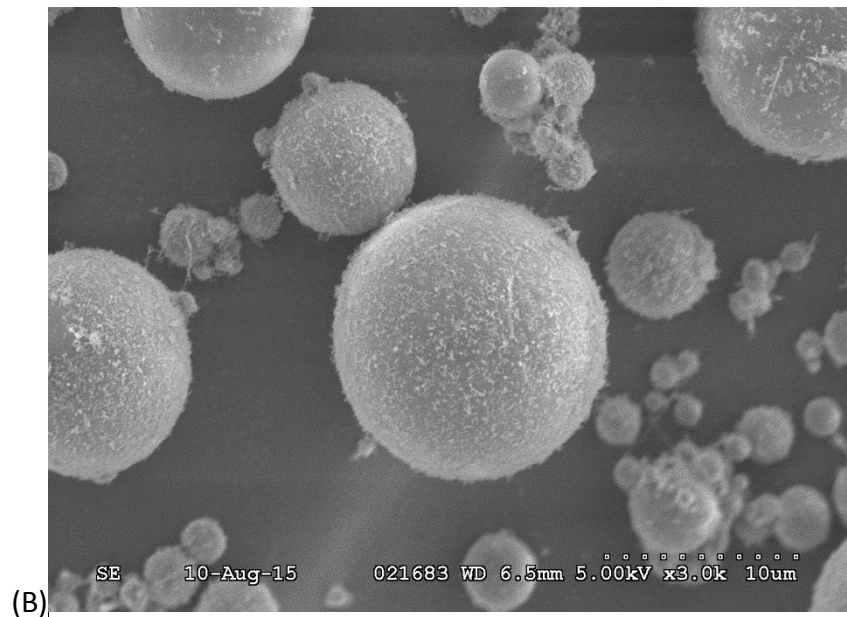
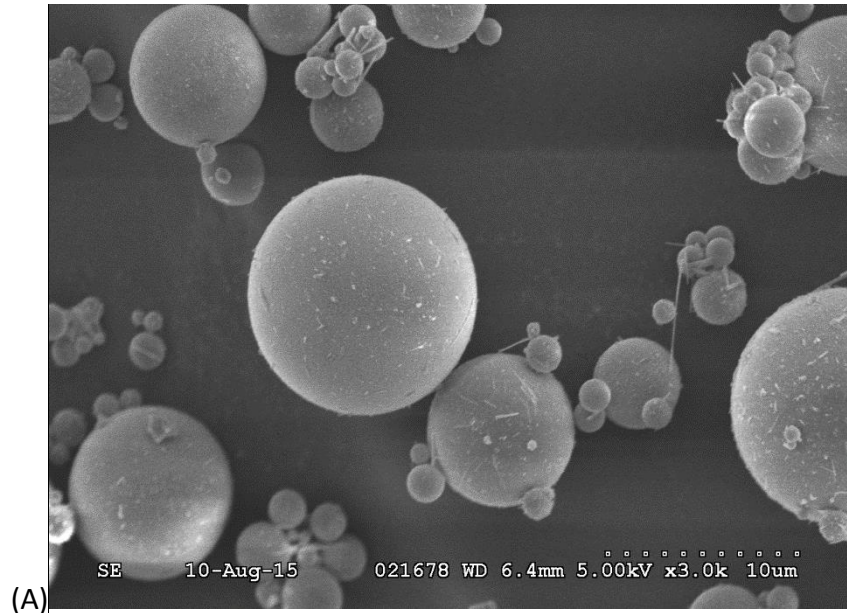
Scanning electron microscopy (S-2600N Scanning Electron Microscope, Hitachi Ltd., JP) is applied to study the surface morphology and surface quality of the resulting particles after mixing. Nanoparticles were blended with host particles by an ultrasonic vibrating method; more details were in the patent (Zhu, J; Zhang, 2006).

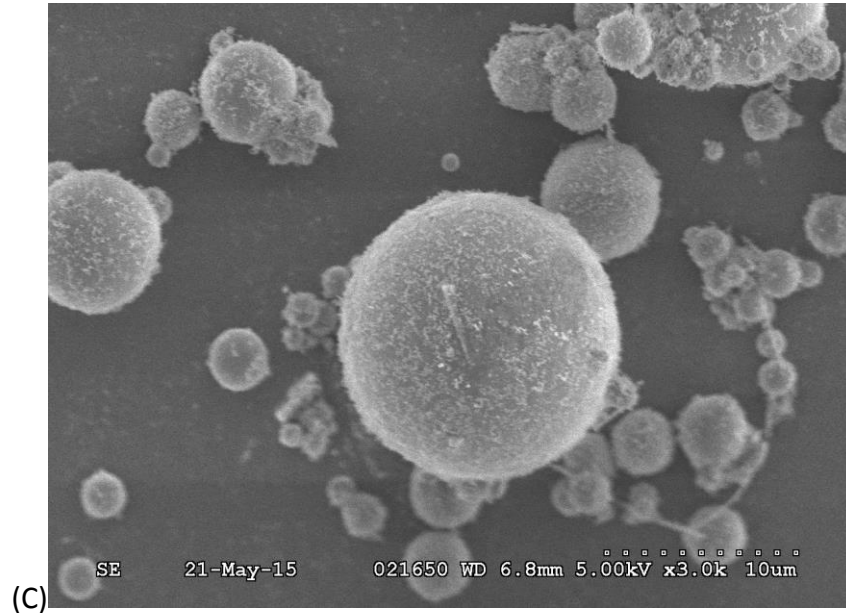
5.1 Surface Modification by Nanoparticles

Figure 5.1 shows the SEM images of glass beads (10 μm), Figure 5.1 (A) and (B) give the images of the particles before and after surface coating, the modification results are obvious: the surface of glass beads virgin particles are smooth and many nature agglomerates exist, due to the inherent strong interparticle forces. After blended with nanoparticles, the surfaces becomes rougher and the nano SiO_2 particles cling onto the glass beads as asperities, and distribute uniform. Also, the absence of these large agglomerates after coating suggests that they can be efficiently broken up into smaller sizes during ultrasonic vibration mixing.

Compared to figure 5.1 (B), the glass beads modified with nanoparticles after two days

fluidization was shown in figure 5.1 (C). Glass beads still covered by nanoparticles which have not fallen off with fluidization time. While, the nanoparticle effect may change by different materials and concentration.





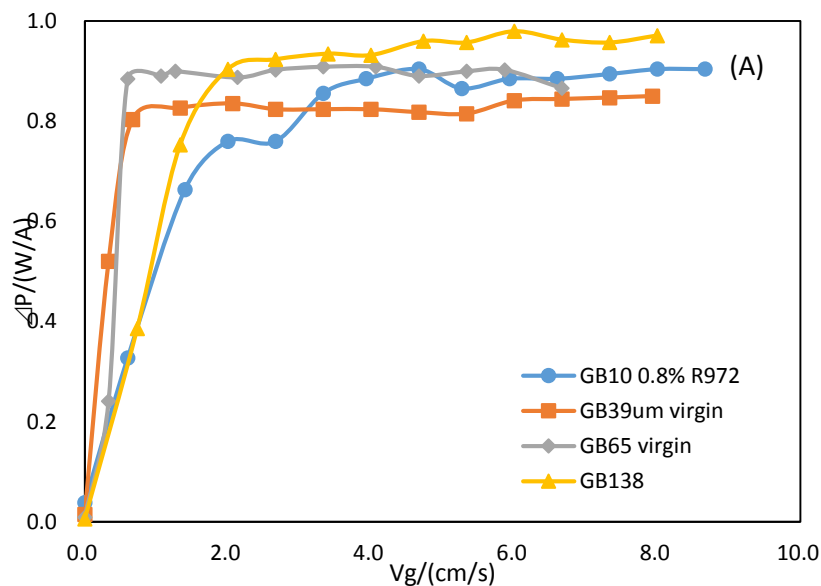
(C) Figure 5.1 SEM image of glass beads 10µm (A) virgin particles (B) GB10 blended with 0.8%w/w R972 (C) GB10 with 0.8%w/w R972 after fluidization

5.2 Fluidization Characterization of Geldart Group C Particles with Nano-additives

Glass beads 10 µm as typical Geldart group C particles, have the character of cohesion and poor fluidization quality, because the strong interparticle force, especially Van der Waals force. 16nm SiO₂ as fluidization aids could successfully improve fine particle fluidization. However, the improved fluidization still has some special fluidization properties compared to Geldart group A particles. Figure 5.2 shows a summarized normalized pressure drop and bed expansion of glass beads 10 µm with 0.8%R972w/w compared to Geldart group A particles.

For glass beads 39, 65 and 138 µm virgin particles, all experienced the traditional fluidization behavior: as superficial gas velocity increases, fluidization starts from fixed bed, conventional fluidized bed, bubbling fluidized bed, turbulent fluidized bed even to circulating fluidized bed. Normally, for Geldart group A particles, small and big bubbles both exist and they changed quickly as gas flow through the whole bed. But for fine

particles, as the effect of nanoparticles, fine particle could be fluidized well and more uniformly without big bubbles. The reduction in bubble size for fine particles could be due to a lower total bubble gas flowrate (Varadie & Grace, 1978). The total bubble gas flowrate is $Q_b = AV_g - Q_D$, where A is bed cross-section area, Q_b is apparent bubble gas flowrate and Q_D is gas flowrate through dense phase. A bubble splits when a curtain of particles which has started from the bubble roof reaches the bubble floor before it is swept around to the equator of the bubble. Small bubbles are not very sensitive to disturbances of wavelengths normally seen in fluid beds. Large bubbles are more sensitive and will be easily split (Clift, Grace, & Weber, 1974). Because of the roof instabilities, fine particles much easier occur this phenomenon which prevent big bubbles exist. In pressure drop profile of glass beads 10 μm with 0.8%w/w R972, when gas velocity is low, particles haven't fluidized immediately, but experienced a period of poor fluidization with agglomerates and channeling, at bed bottom and boundary. Pressure drop increase slowly compared to Geldart group A particles. However, after fine particles fluidization, a little increase of normalized pressure drop indicate that some agglomerates break to single particles in higher gas velocity.



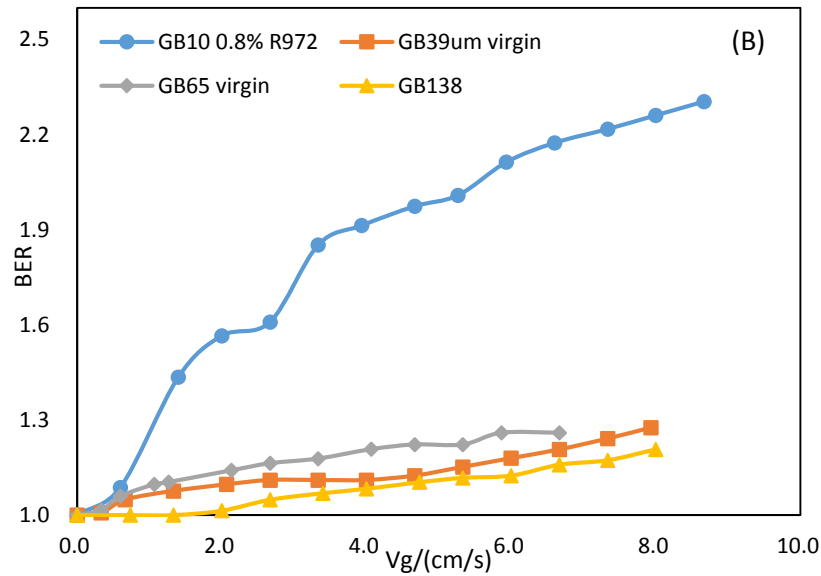


Figure 5.2 Fine particle fluidization with nanoparticles compared to Geldart group A particles (A) Normalized pressure drop (B) Bed expansion

With the variation of nanoparticle concentration, fine particle fluidization behavior are no much difference. When nanoparticles as fluidization aid participated in fine particle fluidization, their fluidization quality improved much no matter what is the additive concentration, from 0.5% to 1.5%w/w. Figure 5.3 reveals the normalized pressure drop and bed expansion of glass beads 10 μm with different nanoparticle concentration. At high gas velocity, all of the normalized pressure drop value of fluidization with nanoparticles close to 1, which means the fully fluidization of whole bed; at lower gas velocity, nanoparticle concentration of 0.5%w/w give a little weak fluidization compared to 0.8% and 1.5% R972, and additive concentration of 0.8% and 1.5% looks similar, normalized pressure drop rise rapidly and stabilize around 0.9.

For bed expansion, after the improvement of fine particle, different nanoparticle concentration don't show much difference in bed expansion, but the bed expansion ratio is much higher than Geldart group A particles, uniform and high bed expansion decide a better gas solid mixing and heat transfer in chemical reaction. As gas velocity increases,

bed expansion keep increasing.

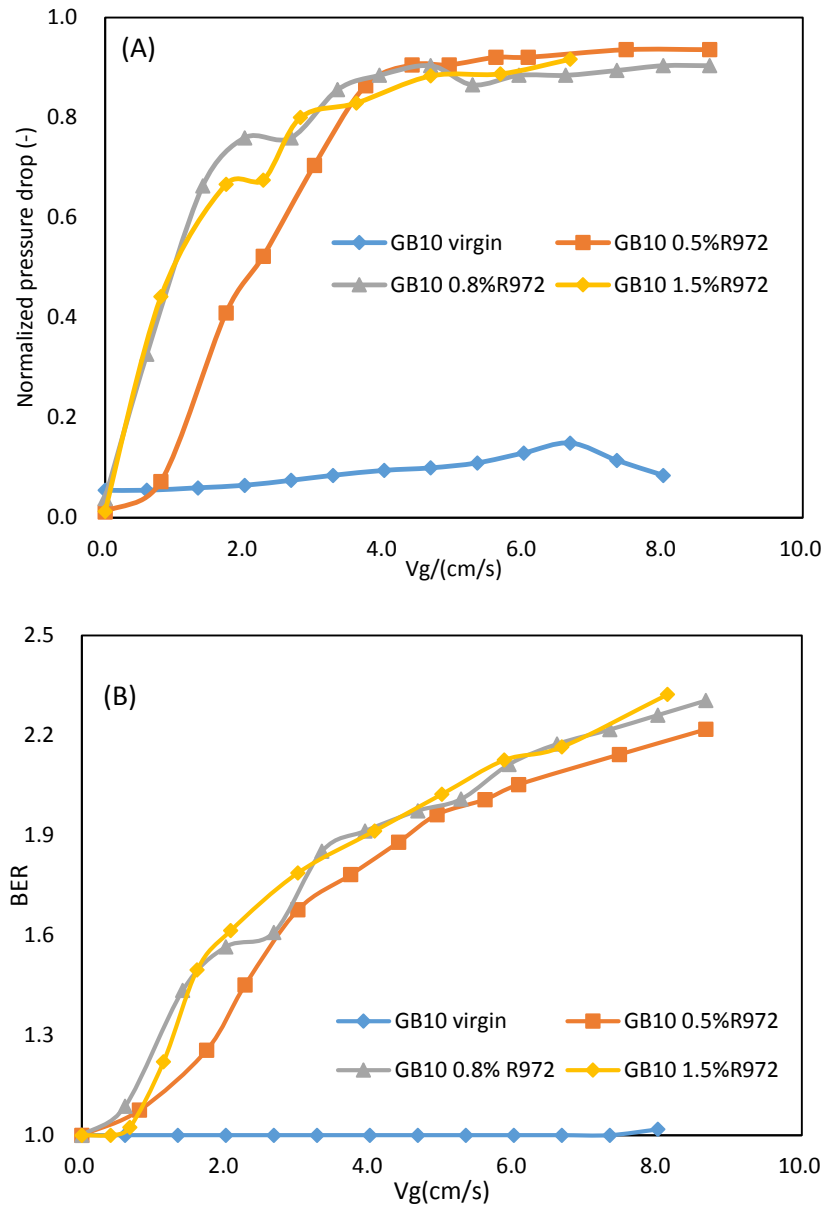


Figure 5.3 Fine particle fluidization with different nanoparticle concentration
(A) Normalized pressure drop (B) Bed expansion ratio

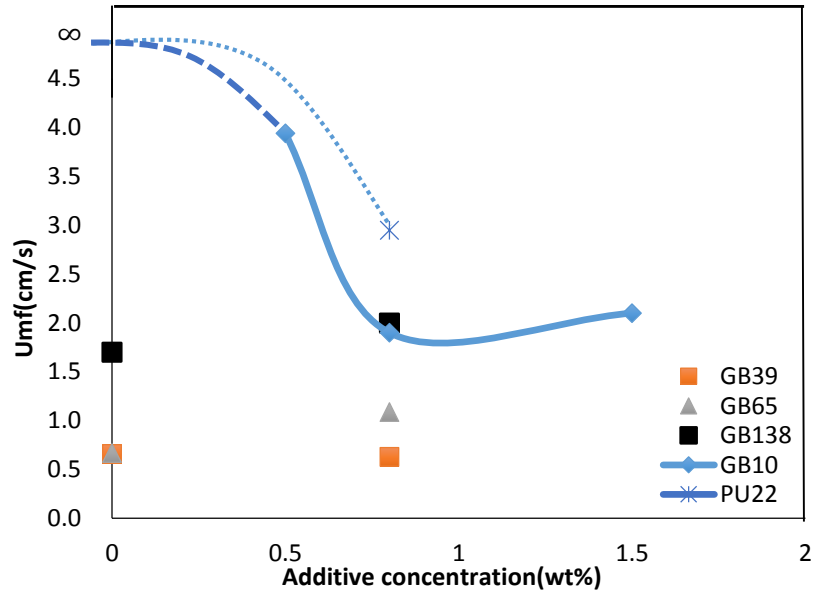


Figure 5.4 The minimal fluidization velocity with different particles

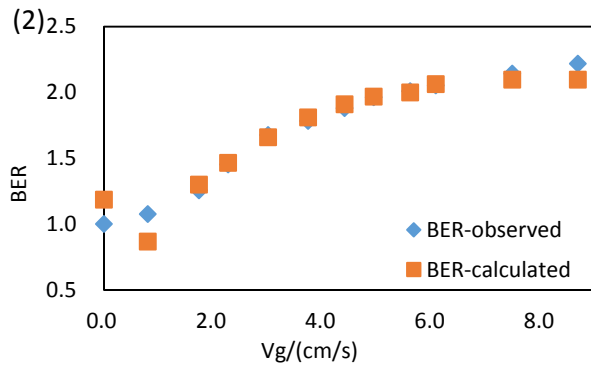
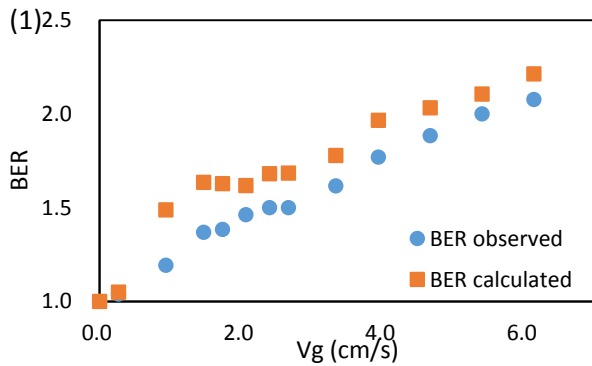
Figure 5.4 shows the minimal fluidization velocity of all the experiment particles. For glass beads 10 μm particle, at the beginning, U_{mf} is infinity because the virgin GB10 is non-fluidization. Then, 0.5%w/w additive play a part and minimal fluidization velocity decrease to 4cm/s, as the additive concentration increase, U_{mf} decrease to 2cm/s but no changes anymore between 0.8% and 1.5%w/w nanoparticles. But for larger particles such GB39, 65 and 138 μm , nanoparticle has no effect on reducing minimal fluidization velocity, even a little goes bad, as least this result indicate nanoparticles have no influence on Geldart group A , when particle size is big enough that Van der Waals force was not a dominant factor on particle cohesive property.

5.3 Discussion on Bed Height Test

In a fluidized bed, bed expansion always changed from time to time, particles moved with gas flow, so bed height fluctuate in a certain range. It's hard to ensure the accuracy of bed height observation. Another bed height test method is the bed height calculated from pressure drop. The precondition of calculated equation is the good fluidization when the

whole bed density is stable, and the smoother the dispersion, the more precise.

Figure 5.5 shows the 8 bed expansion ratios tested by the two methods. The first four figures expressed the BER of particles related to Geldart group C, PU and GB with additives. The last four reveals the larger particle with or without nanoparticles. Obviously, the BER of fine particles from calculation and observation were remarkably consistent, which means the observation results of fine particle is correct and enough precise. Another perspective is, when fine particle is fluidized, bed height fluctuation is not significant, and instead, the tiny change indicate more uniform particle dispersion and ignorable bubble influence. The smooth and stable fluidization also ensure the calculated accuracy. But for Geldart group A particles, at lower gas velocity, the two method results could correspond to each other, because these particles fluidized quickly and bed height variation inconspicuous. With the increasing of gas velocity, the divergence occurred of these two method values, big bubbles results in a variable fluidized bed density and huge bed height fluctuation.



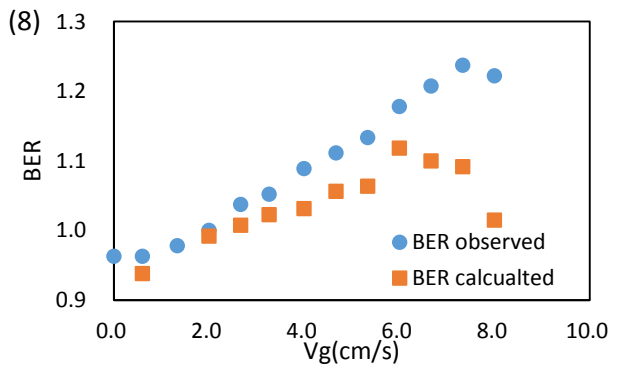
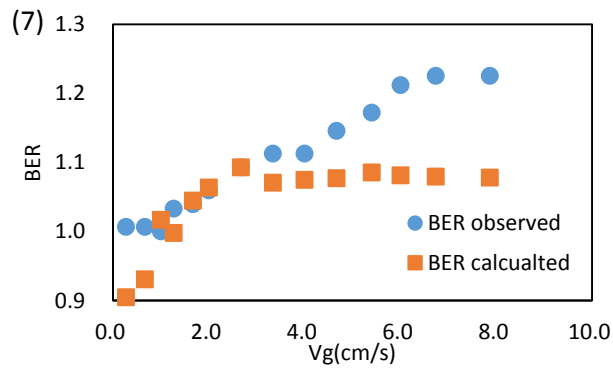
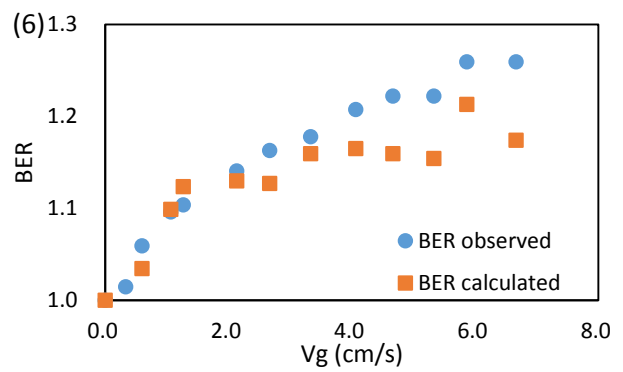
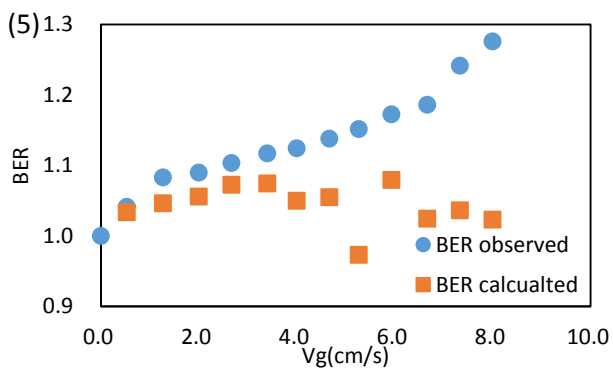
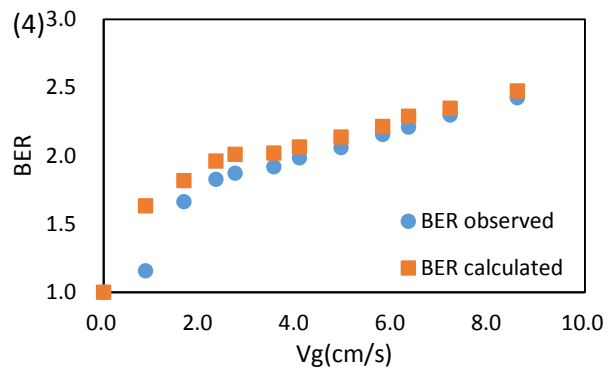
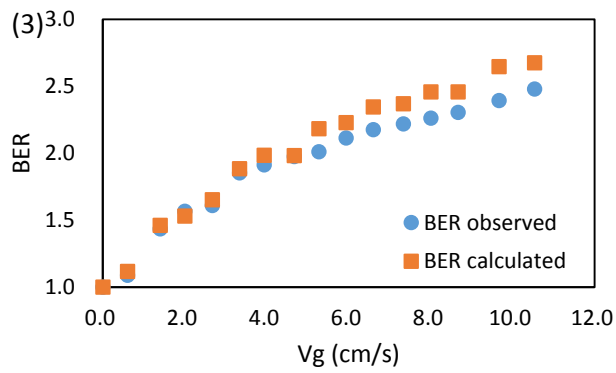


Figure 5.5 BER of two test method

- (1) PU22+0.8%R972 (2) GB10+0.5%R972 (3) GB10+0.8%R972 (4) GB10+1.5%R972
 (5) GB39 virgin (6) GB65 virgin (7) GB65+0.8%R972 (8) GB138+0.8%R972

5.4 Conclusion

The SEM microscopy verified the nanoparticle effect and durability in fine particle fluidization. When fine particle fluidization have been improved by nanoparticles, their

fluidized behavior is similar with Geldart group A particles, such as fluidization experience started from fixed bed to circulating with gas velocity increase. But the improved fine particle fluidization are still slower to fluidized, compared to larger particles. However, at high gas velocity, bed expansion could reach 2-3 times of fixed bed, and more uniform particle dispersion occurs in gas solid fluidization.

For nanoparticle concentration, although the optimum additive concentration must exist, but nanoparticle effect of fine particle fluidization had little difference on the characterization of pressure drop and bed expansion. For another, nanoparticle is helpful on fine particle fluidization, but the effect of Geldart group A particle looks inconspicuous, even shows a negative influence.

The results of two bed expansion test methods identify the accuracy of bed height observation for fine particles, also shows a uniform dispersion and stable fluidized bed density, and indicates small bubble size in no matter low or high gas velocity. For large size particle, big bubbles exist and local fluidized bed density is always changed, so the calculated method is not suitable, but as the large particles are less cohesive, the observation of bed height is much easier than Geldart group C.

Nomenclature

A	Bed cross-section area, [cm ²]
V_g	Superficial gas velocity, [cm/s]
U_{mf}	Minimal fluidization velocity, [cm/s]
Q_b	Apparent bubble gas flowrate, [cm ³ /s]
Q_D	Gas flowrate through dense phase, [cm ³ /s]
I.D.	Inside diameter

Bibliography

- Baerns, M. (1966). Effect of interparticle adhesive forces on fluidization of fine particles. *Industrial & Engineering Chemistry Fundamentals*. Retrieved from <http://pubs.acs.org/doi/abs/10.1021/i160020a013>
- Chaouki, J., Chavarie, C., Klvana, D., & Pajonk, G. (1985). Effect of interparticle forces on the hydrodynamic behaviour of fluidized aerogels. *Powder Technology*, 43(2), 117–125. [http://doi.org/10.1016/0032-5910\(85\)87003-0](http://doi.org/10.1016/0032-5910(85)87003-0)
- Clift, R., Grace, J., & Weber, M. (1974). Stability of bubbles in fluidized beds. *Industrial & Engineering Chemistry* Retrieved from <http://pubs.acs.org/doi/abs/10.1021/i160049a009>
- Geldart, D. (1973). Types of gas fluidization. *Powder Technology*, 7(5), 285–292. [http://doi.org/10.1016/0032-5910\(73\)80037-3](http://doi.org/10.1016/0032-5910(73)80037-3)
- Gibilaro, L. G. (2001). *Fluidization Dynamics*. Butterworth-Heinemann. Retrieved from <https://books.google.com/books?id=RIZutdBfY4sC&pgis=1>
- Krupp, H. (1967). Particle adhesion, theory and experiment. Retrieved from https://scholar.google.ca/scholar?q=particle+adhesion+theory+and+experiment&btnG=&hl=en&as_sdt=0%2C5#0
- Lauga, C., Chaouki, J., Klvana, D., & Chavarie, C. (1991). Improvement of the fluidisability of Ni/SiO₂ aerogels by reducing interparticle forces. *Powder Technology*. Retrieved from <http://www.sciencedirect.com/science/article/pii/003259109180208Z>
- Pacek, A. W., & Nienow, A. W. (1990). Fluidisation of fine and very dense hardmetal powders. *Powder Technology*, 60(2), 145–158. [http://doi.org/10.1016/0032-5910\(90\)80139-P](http://doi.org/10.1016/0032-5910(90)80139-P)
- Varadie, T., & Grace, J. R. (1978). High pressure fluidization in a two-dimensional bed, in Fluidization. In *Proceedings 2nd Engineering Conference*, ed. JF Davidson and DL Keairns (pp. 55–58). Cambridge University Press.
- Visser, J. (1989). Van der Waals and other cohesive forces affecting powder fluidization. *Powder Technology*, 58(1), 1–10. [http://doi.org/10.1016/0032-5910\(89\)80001-4](http://doi.org/10.1016/0032-5910(89)80001-4)
- Zhou, T., & Li, H. (1999). Effects of adding different size particles on fluidization of cohesive particles. *Powder Technology*. Retrieved from

<http://www.sciencedirect.com/science/article/pii/S0032591098002113>

Zhu, J; Zhang, H. (2006, February 1). Method and apparatus for uniformly dispersing additive particles in fine powders. Retrieved from <https://www.google.com/patents/US7878430>

Chapter 6

Further Investigation on Dense Phase Expansion

A special characterization of fine particle fluidization is the bed expansion improvement. A higher bed expansion generally indicates a better fluidization with more gas contained in the particulate phase, resulting in better gas solid contact (Wang et al., 1998). But the stronger interparticle forces allow the micro-voids to increase in number or size (Geldart, Harnby, & Wong, 1984). Regarding to bubble-free fluidization of cracking catalysts (Massimilla, Donsi, & Zucchini, 1972), it has been shown that bubble-free fluidized beds contain cavities and micro-channels. Bed expansion of fine particles occurred primarily by the nucleation and growth of cavities or particle defects (Donsi & Massimilla, 1973). There are significant differences between the expansion of a cohesive powder and that of a Group A powder: the visual appearance of the beds is quite different, few bubbles can be seen and horizontal/sloping cracks appear. The occasional small bubbles seen at the wall of a cylindrical bed “wipes out” any cracks in its path and the cracks re-form with a different inclination and length. Vertical channels are also seen, particularly at the bed surface. When they first form they resemble volcanoes out of which particles are ejected; if they stabilize activity appears to cease and only gas comes out (Geldart & Wong, 1985).

After fluidization aids, bed expansion of fine particles increased quickly and dispersed homogeneously. The research of bed expansion after fluidization aids is lack of study. A series of Geldart group C particles were used in this experiment, to investigate nanoparticle concentration and particle size influence of bed expansion. Moreover, bed collapse test corresponding to different gas velocities exhibit more clear bed expansion behavior.

Bed collapse test is a very useful tool to analyze the details of bed expansion. In a

collapsing gas solid fluidized bed, after the gas flow has been suddenly cut off, the gas flow can be divided into three components (Tung, Yang, & Xia, 1989): 1) via bubble translation and throughflow; 2) through the interstices of suspended particles; 3) driven out by the consolidating particles. During the collapse of the bed of particles, all three types of gas flow take place simultaneously. After the gas supply to a bubbling bed is shut off, bubbles ascend through the bed and leave through the surface of the bed. This is the bubble escape stage. The bed level drops quickly during this period. At the end of the bubble escape stage, the gas flow through the interstices of suspended particles becomes predominant. This is the hindered sedimentation stage. The bed collapse rate is constant and slower than for the bubble escape stage. The end of the hindered sedimentation stage is the beginning of the solid consolidation stage. During the solid consolidation stage, the bed has uniform density. The gas in the interstitial space is expelled by the accumulation of particles. The rate of bed collapse is relatively slow (Abrahamsen & Geldart, 1980b).

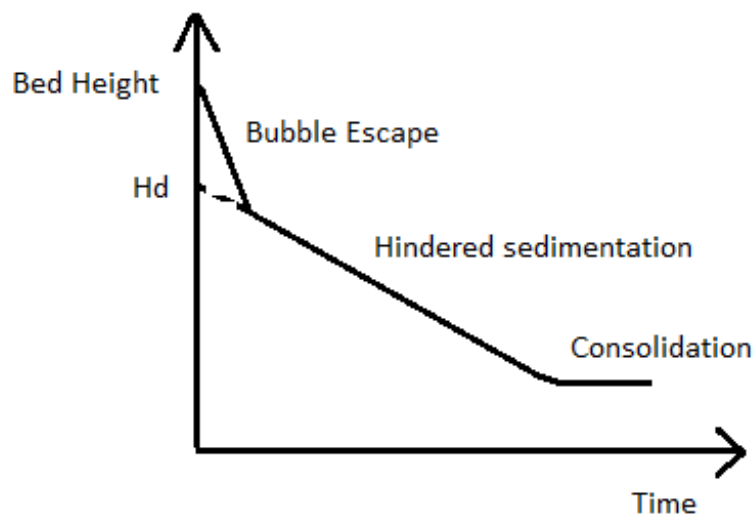


Figure 6.1 typical bed collapse test curve

An example is shown on Figure 6.1, if the hindered sedimentation stage is extrapolated to time zero, where the intercept on the ordinate axis is the dense phase bed height. The

dense phase voidage can then be calculated by mass balance. Table 6.1 gives the particle properties in this experiment.

Table 6.1 Physical properties of experimental particles

Powder Name	Particle Size (μm)	Material	Shape	Particle Density (kg/m^3)	Bulk Density (kg/m^3)	Geldart Powder Classification
Glass beads	6	Soda-lime-Silica glass	Spherical	2500	704.1	C
Glass beads	10	Soda-lime-Silica glass	Spherical	2500	738.3	C
Talc	18.5	hydrous magnesium silicate	Irregular	2750	712.7	C
PU	22	Polyurethane	Irregular	1200	689	C
Glass beads	39	Soda-lime-Silica glass	Spherical	2500	1301.2	A
Glass beads	65	Soda-lime-Silica glass	Spherical	2500	1254	A
Glass beads	138	Soda-lime-Silica glass	Spherical	2452.6	1421	A

6.1 Influence of Nanoparticles on Different Particle Size

Nanoparticles as a kind of fluidization aids could improve the fluidization behavior of fine particles. In Geldart particle classification, fine particle means particle size below $30 \mu\text{m}$, while, the nanoparticle effect of different particle size was not much investigated. Figure 6.2 shows the bed expansion influence of nanoparticle in different particle size ranged from 6 to $65 \mu\text{m}$.

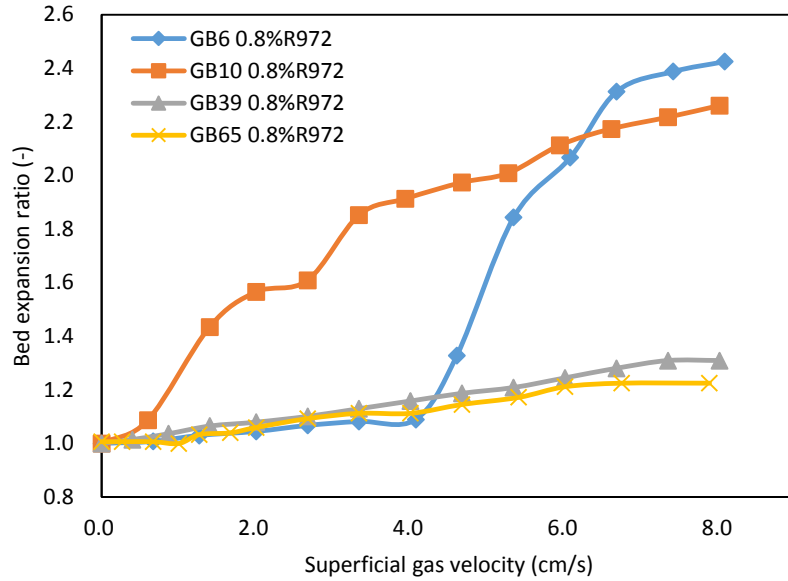


Figure 6.2 Bed expansion with nanoparticle of different particle size

Regarding to fine particle such as GB6 and GB10, when fluidization occurs with nanoparticles, bed expands much higher. Because the cohesive property inhibited gas flowing out the bed; and the small particle size in lighter weight ensured more particle number held in the whole bed, when we keep the same weight of each samples. This two main reasons indicate a 2-3 times bed expansion of fine particles. However, for GB39 and GB65, BER only reached to 1.2, because the bigger particle size leads to heavier particle weight, so that single particles are not easily suspended, when gas flowrate increased. The redundant gas flew out of the bed fast, bubbles emerged and broke, particles are flew up and down, moved in circles. Bed expansion were not changed with increasing gas velocity. While, the density of glass beads inherently much heavier than gas density, for the lighter particles whose density related to air may occur another phenomenon.

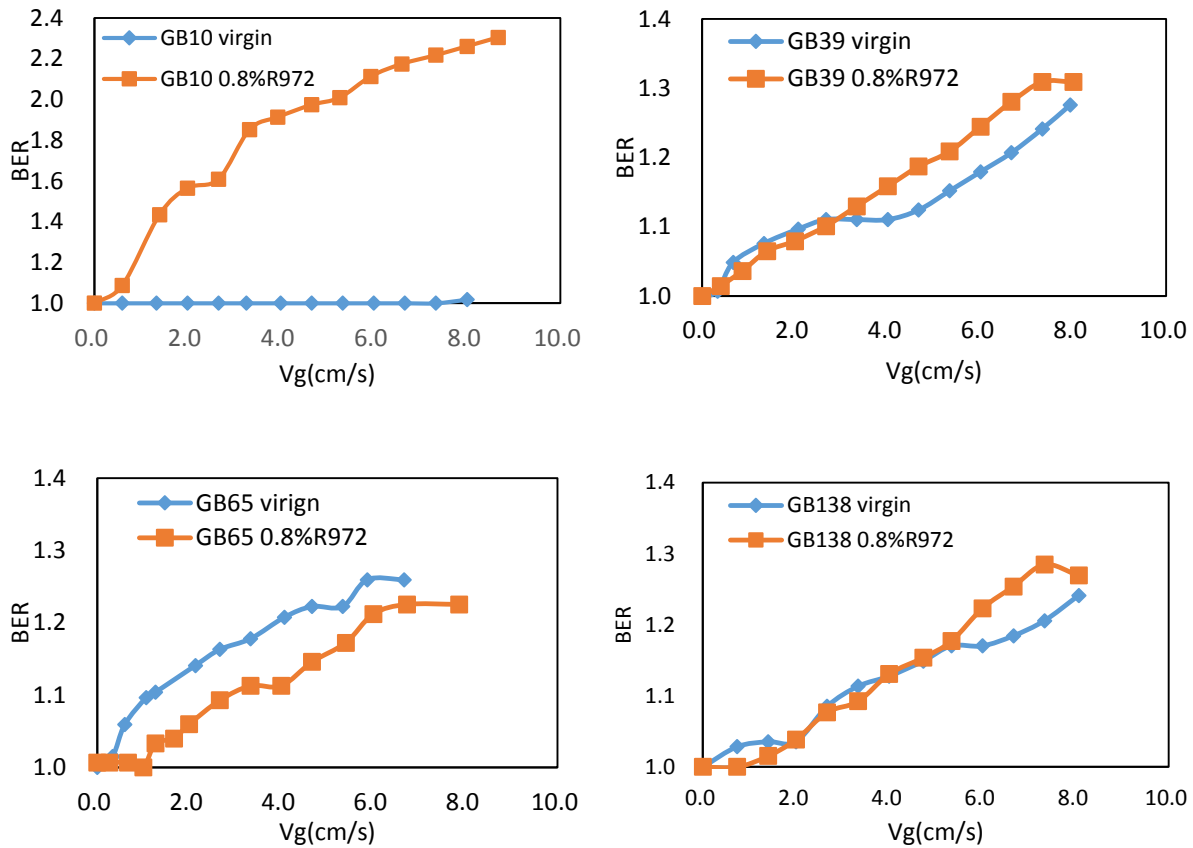


Figure 6.3 Nanoparticle effect of BER respect to different particle size

Compared to fine particle fluidization, nanoparticle effect of larger particles reveals neither better nor worse. Figure 6.3 clarify the summary of nanoparticle effect of different size particles. The larger particles could exist in form of single particles in a fluidized bed, when nanoparticles added and mixed with virgin particles, nanoparticle also coated on the host particle surface, however, Geldart group A particles could be fluidized well itself, nanoparticle has no effect on larger particle fluidization enhancement. For another, the significant bed expansion of fine particles is because of itself smaller particle size, but not nanoparticles as fluidization aids.

6.2 Bed Collapse Test

Beside bed expansion test, another striking difference between Geldart group A and C particles is the results of the bed collapse test (Geldart et al., 1984). The typical Geldart group A particles bed collapse curve was shown in Figure 6.1. Figure 6.4 shows the bed collapse test of a typical Geldart group C glass beads 10 μm , both samples are shut down at 10cm/s superficial gas velocity. GB10 virgin particles are difficult to fluidize, although at high gas flowrate, the bed expansion only reached to 1.4, but after the gas supply shut off, there is no bubble escape stage, but directly experience the second stage, the hindered sedimentation. Gas escape from cohesive particles and bed height slowly fall off, and the time of sedimentation is almost same as the other samples with nanoparticles. For glass beads 10 μm with nanoparticles, the bubble escape stage only lasts 1 second, because glass beads particles are much heavier, a few particles in bubble phase dropped off in a second and gas escaped from bubble phase, when gas supply shut off; but bed collapse experiences almost 40 seconds at the second stage. Then bed collapse access to sedimentation stage. Much micro-voids kept between finer particles, as fine particles are very cohesive and easier to form agglomerates, the gas in dense phase were hindered to flee away, so bed height reduced slowly.

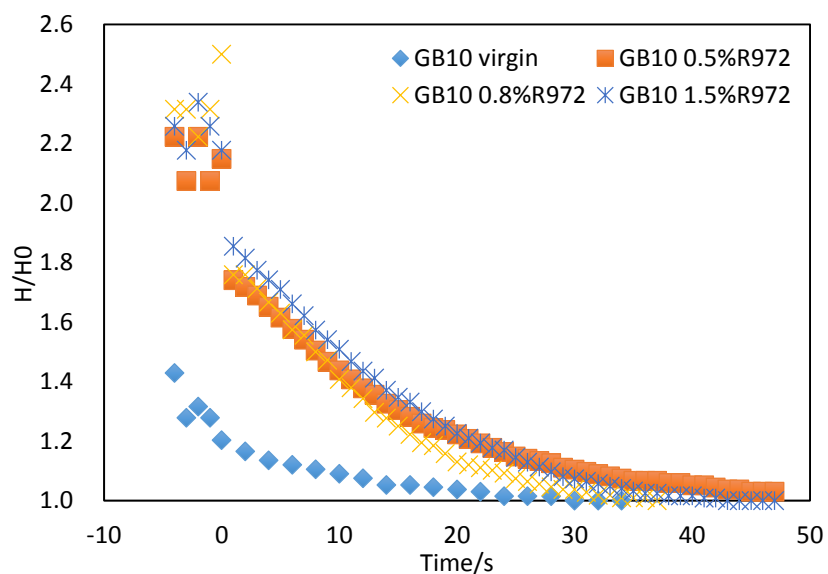


Figure 6.4 Bed collapse test of GB10

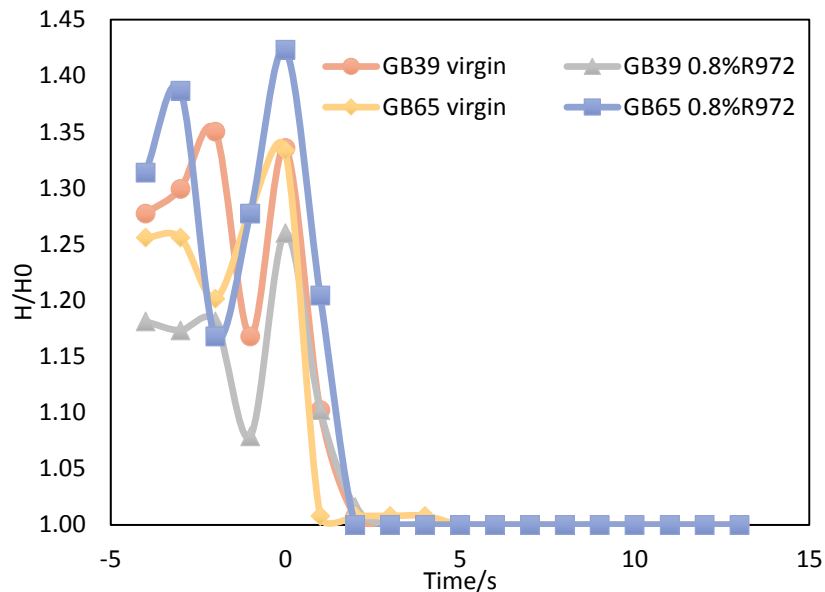


Figure 6.5 Bed collapse test of GB39 and GB65

However, for larger size particles, bed height fluctuate wildly because of big bubbles, bed expansion only reached to 1.4, after the gas supply shut down, bubble escapes in 2 seconds and the sedimentation and consolidation were hard to observe, shown in Figure 6.5. Whether the virgin particles or particles with additives, bed height and bed collapse curve almost no differences, which also imply the poor effect of nanoparticle respect to larger particles.

6.4 Bed Collapse Dense Phase

The bed collapse technique has been used to evaluate the average dense phase properties in vigorously fluidized beds of fine particles (Abrahamsen & Geldart, 1980a). In bed collapse curve, if the hindered sedimentation stage is extrapolated to time zero, where the intercept on the ordinate axis is the dense phase bed height, and the dense phase voidage can then be calculated by mass balance. Figure 6.6 shows the dense phase voidage calculated by collapse test curve of 4 kinds of fine particles. As we discussed

before, fine particles have a high dense phase bed height compared to Geldart group A particles. A higher dense phase voidage indicates a more gas friction in dense phase. The calculation equation is below:

$$\varepsilon_d = 1 - \frac{(1-\varepsilon_0)H_0}{H_d} \quad (6.2)$$

Where ε_d is dense phase voidage, ε_0 is voidage at normal state, H_d is dense phase bed height and H_0 is fixed bed height.

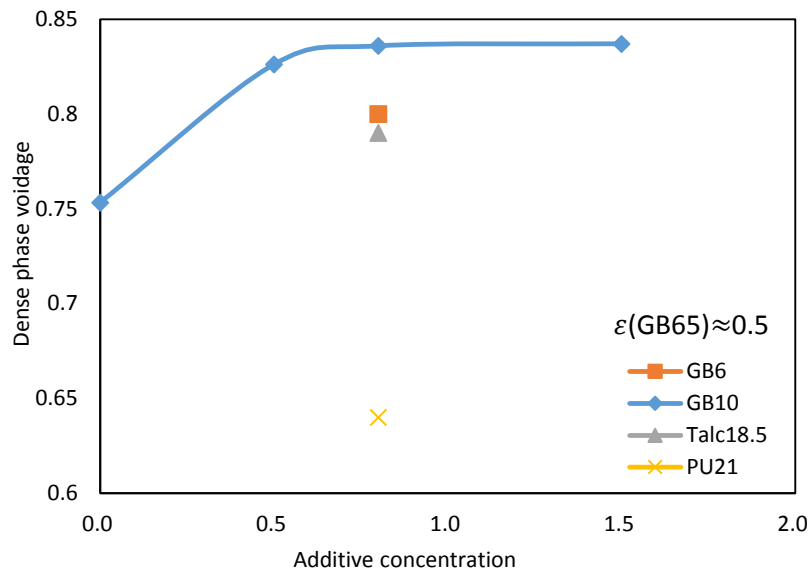


Figure 6.6 Dense phase voidage of 4 kinds of fine particles

For different particle density, glass beads and talc express a high dense phase compared to polyurethane. A reasonable explanation may be from surface energy. Glass beads and talc both contain the silica material, additive also is SiO_2 , the surface energy of silica-silica is much higher than silica-PU (Clint & Dunstan, 2001), so when gas supply shut down in bed collapse test, the high surface energy particles have a strong obstruction to hinder gas flow away from dense phase, which decide a higher dense phase bed height, and then dense phase voidage as well. Although the dense phase voidage of PU is relatively lower, the bed height growth factor is pretty high, this phenomenon reveals bubble phase is

significant in bed expansion of polyurethane. As additive concentration increases, dense phase voidage increases at beginning and then hold the line. Taken in this sense, the best nanoparticle concentration is around 1%w/w, and additive improvement of dense phase voidage is about 0.1.

6.5 Influence of Gas Velocity on Bed Collapse Test

The investigation of different shut down gas velocity in bed collapse test were studied. The typical fine particle glass beads 10 μm with 0.8%R972 were chosen in this experiment. The lowest velocity was chosen the minimal fluidization velocity. In Figure 6.7, an obvious difference was the bubble phase appearance and increase. At lowest gas velocity, no bubble escape phase exist, the bed collapse curve directly passed into sedimentation stage; as shut off gas velocity increased, bubble phase occurred and the height of bubble escape rose up. Another significant phenomenon was that the sedimentation stage almost experienced the same time no matter what is the gas velocity and dense phase bed height.

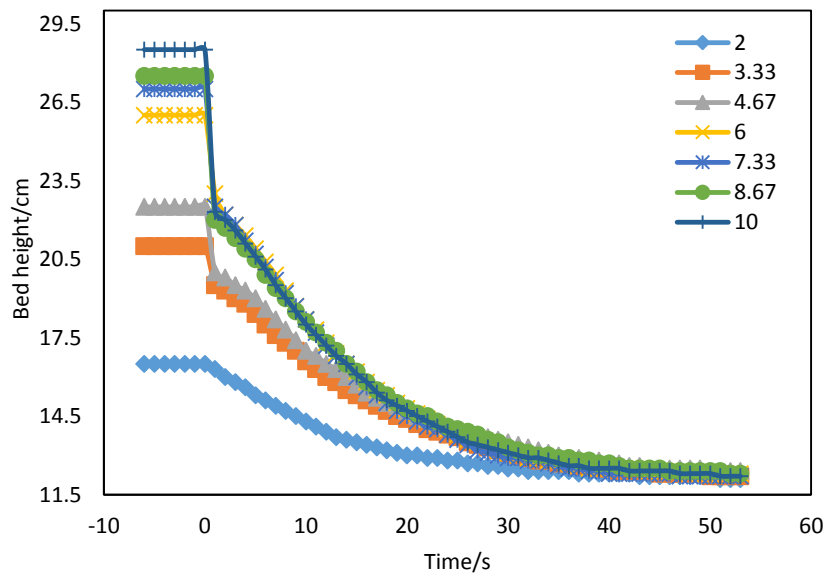


Figure 6.7 GB10 with 0.8%R972 bed collapse test in different gas velocity

Figure 6.8 expressed the dense phase voidage calculated from figure 6.9. Firstly, the variation of lowest to highest of dense phase voidage is around 0.1, which is important for heat and mass transfer especially in industry. In addition, when gas velocity increase to a certain value, in this experiment was 6cm/s, the dense phase voidage were not changed anymore.

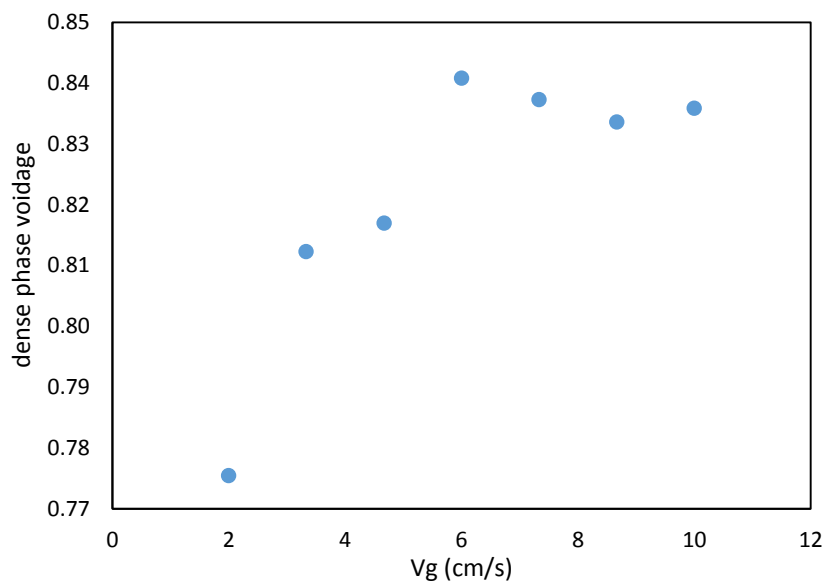


Figure 6.8 Dense phase voidage of different shut down gas velocity

6.6 Bed Height Growth Factor

In this investigation, we defined a new parameter, bed height growth factor (R_G), to express the particle expansion ability. When Geldart group A particles fluidized, bed height fluctuate wildly but always kept on an unchanged level, while the bed height of fine particle fluidization was a little increasing with increased gas velocity. The bed expansion keep increasing after minimal fluidization velocity of fine particle fluidization may be caused by two reasons. One is that more fine particles formed as agglomerates before break up expanded with increasing gas velocity, the pressure drop profile could verify this

inconspicuous phenomenon. The pressure drop still keep a little growth after minimal fluidization velocity, but the growth rate is pretty low even negligible. Another main reason is that fine particles have the ability of hold more air during fluidization. Therefore, the bed height growth factor is defined as the bed height growth ratio after minimal fluidization. The equation is as follow:

$$R_G = 100 \frac{BER_{final} - BER_{U_{mf}}}{U_{final} - U_{mf}} \quad (6.1)$$

Actually, bed height growth factor is the slope of BER after minimal fluidization. But we designed a coefficient, for revising unit to $(m/s)^{-1}$, and enlarging the range of R_G .

Figure 6.9 reveals the R_G respect to five kinds of particles with different nanoparticle concentration. Obviously, larger size particles such as GB39, 65 and 138, although the particle size difference should not be ignored, their R_G were almost same, either with or without nanoparticles, which indicate the weak ability of gas “dissolve” in particle fluidization. But for finer particles, the high R_G implies high bed expansion and good gas dissolve ability. The curve of glass beads 10 μm reveals the improved trend with increased additive concentration, polyurethane 22 μm with nanoparticle also has a high bed height growth factor. The higher R_G indicate a better gas solid mixing, and mass and heat transfer.

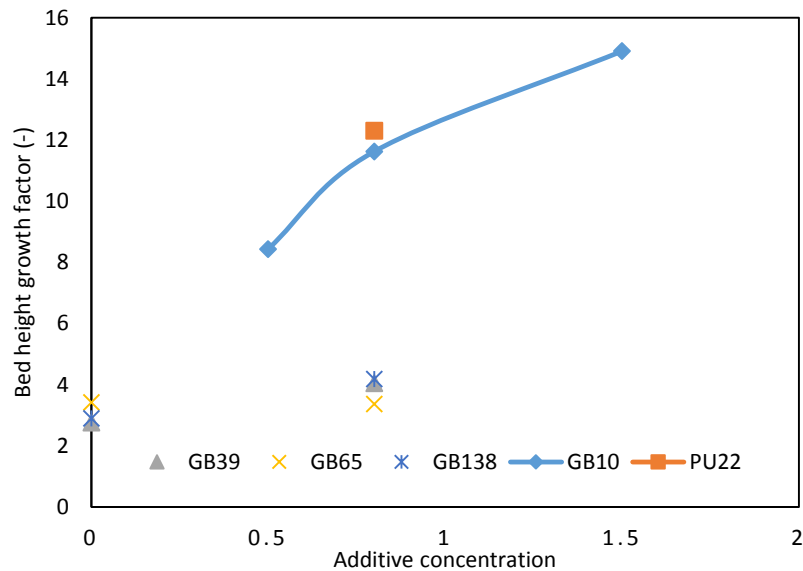


Figure 6.9 Bed height growth factor of experimental particles

6.7 Conclusion

Fine particles have a significant fluidization character which is 2-3 times bed expansion. A higher bed expansion generally indicates a better fluidization with more gas contained in the particulate phase, resulting in better gas solid contact. With fluidization aids, fine particles bed expansion improved much higher, because the cohesive property of fine particles inhibited gas flowing out of the bed, but for Geldart group A particles, nanoparticles influence were unobvious.

Fine particles collapse curve were different with the typical bed collapse, a large sedimentation stage decided the high dense phase compared to Geldart group A. Superficial gas velocity was an important factor to effect dense phase bed height. But when gas velocity up a certain value, dense phase height no longer increase, this phenomenon could use to find the optimum velocity, keeping suitable dense phase.

When fine particle fluidized, bed expansion keep increasing with gas velocity goes up. A

new dimensionless parameter named bed height growth factor (R_G) were introduced to express particle expansion ability, and R_G is defined as the slope of BER after minimal fluidization. With additive concentration increase, increasing bed height growth factor indicated the positive effect of nanoparticles on bed height growth.

Nomenclature

R_G	Bed height growth factor, [-]
H_0	Initial bed height, [cm]
H_d	Dense phase bed height, [cm]
U_{mf}	Minimal fluidization velocity, [cm/s]
BER	Bed expansion ratio, [-]

Greek letter

ε_d	Dense phase voidage, [-]
ε_0	Particle voidage at static state, [-]

Bibliography

- Abrahamsen, a. R., & Geldart, D. (1980a). Behaviour of gas-fluidized beds of fine powders part I. Homogeneous expansion. *Powder Technology*, 26(1), 35–46. [http://doi.org/10.1016/0032-5910\(80\)85005-4](http://doi.org/10.1016/0032-5910(80)85005-4)
- Abrahamsen, a. R., & Geldart, D. (1980b). Behaviour of gas-fluidized beds of fine powders part II. Voidage of the dense phase in bubbling beds. *Powder Technology*, 26(1), 47–55. [http://doi.org/10.1016/0032-5910\(80\)85006-6](http://doi.org/10.1016/0032-5910(80)85006-6)
- Clint, J. H., & Dunstan, T. S. (2001). Acid-base components of solid surfaces and the triboelectric series. *Europhysics Letters (EPL)*, 54(3), 320–322. <http://doi.org/10.1209/epl/i2001-00244-6>
- Donsì, G., & Massimilla, L. (1973). Bubble-free expansion of gas-fluidized beds of fine particles. *AIChE Journal*, 19(6), 1104–1110. <http://doi.org/10.1002/aic.690190604>
- Geldart, D. (1973). Types of gas fluidization. *Powder Technology*, 7(5), 285–292. [http://doi.org/10.1016/0032-5910\(73\)80037-3](http://doi.org/10.1016/0032-5910(73)80037-3)
- Geldart, D., Harnby, N., & Wong, A. C. (1984). Fluidization of cohesive powders. *Powder Technology*. [http://doi.org/10.1016/0032-5910\(84\)80003-0](http://doi.org/10.1016/0032-5910(84)80003-0)
- Geldart, D., & Wong, a. C. Y. (1985). Fluidization of powders showing degrees of cohesiveness—II. Experiments on rates of de-aeration. *Chemical Engineering Science*, 40(4), 653–661. [http://doi.org/10.1016/0009-2509\(85\)80011-7](http://doi.org/10.1016/0009-2509(85)80011-7)
- Massimilla, L., Donsì, G., & Zucchini, C. (1972). The structure of bubble-free gas fluidized beds of fine fluid cracking catalyst particles. *Chemical Engineering Science*, 27(11), 2005–2015. [http://doi.org/10.1016/0009-2509\(72\)87059-3](http://doi.org/10.1016/0009-2509(72)87059-3)
- Tung, Y., Yang, Z., & Xia, Y. (1989). Assessing fluidizing characteristics of powders. ... *on Fluidization*. Retrieved from https://scholar.google.ca/scholar?hl=en&as_sdt=0,5&q=Tung+1989+bed+collapse+fluidization#2
- Wang, Z., Kwauk, M., & Li, H. (1998). Fluidization of fine particles. *Chemical Engineering Science*, 53(3), 377–395. [http://doi.org/10.1016/S0009-2509\(97\)00280-7](http://doi.org/10.1016/S0009-2509(97)00280-7)
- Zhu, J. (2003). Fluidization of fine powders. *Granular Materials: Fundamentals and Applications*, 270–295. <http://doi.org/10.1007/978-94-007-5587-1>

Chapter 7 Conclusions and Recommendations

7.1 Conclusions

This study investigated the several aspects of flow and fluidization fundamentals of fine particles mixed with nanoparticles as flow conditioner (i.e., pressure drop, bed expansion and collapse test, minimal, fluidization velocity), and characterization of powder flowability. In addition, the influence of nanoparticles as fluidization aids and special bed expansion improvement of fine particles have also been conducted.

Cohesion, angle of repose and avalanche angle were applied to measure the flowability of particles from static to dynamic. Nanoparticles as a flow aid blended into host particle to ensure the improved flow behavior, while the improvement is in a certain range which can't change the inherent powder characterization. With the particle size increasing, their angle of repose, avalanche angle and cohesion value were still lower, indicating a better flowability, than fine particles mixed with nanoparticles. The different characterization methods respect to additive concentration shows the same tendency, but different optimum nanoparticle concentration.

In the preliminary study of fluidization behaviors of fine particles with and without additives, the awareness of particle size management, additive influence on different particle size and density, and fluidization characterization of fine particle with additives, all have some interesting breakthrough. As fluidization time goes on, fine particles without nanoparticles reveal an improved fluidization behavior. In the fine particle size distribution, smaller particles are easily blow away so that the particle size would be changed, and the escape of finer particles result in a reduced cohesiveness, until a certain point, these particles could be fluidized well without fluidization aids. Nanoparticles as flow conditioner do have the ability to improve fine particle fluidization quality, but this

improvement could not eliminate channeling, agglomerates or other poor fluidization behavior.

For fine particle with fluidization aids, the results of decreasing flowrate pressure drop test method always could reach a little higher than increasing flowrate method. As fine particle could restrain bubbles generation, the uplift phenomenon in increasing flowrate method is hard to be observed. Two bed expansion test methods, direct observation and calculation from pressure drop, identify the accuracy of bed height observation for fine particles, also shows a uniform dispersion and stable fluidized bed density, and indicates small bubble size in no matter low or high gas velocity. For larger size particle, big bubbles exist and local fluidized bed density is always changed, so the calculated method is not suitable, but as the large particles are less cohesive, the observation of bed height is much easier than Geldart group C.

When fine particles fluidization have been improved by nanoparticles, their fluidized behavior is similar with Geldart group A particles, such as fluidization experience started from fixed bed to circulating with increasing gas velocity. But the improved fine particle fluidization are still slower to fluidized, compared to larger size particles. Regarding to the different nanoparticle concentration, although the optimum additive concentration must exist, nanoparticle effect of fine particle fluidization had little difference on the characterization of pressure drop and bed expansion. For another, nanoparticle is helpful on fine particle fluidization, but the effect of Geldart group A particles look inconspicuous, even show a negative influence.

Fine particles have a significant fluidization character which is the 2-3 times bed expansion. A higher bed expansion generally indicates a better fluidization with more gas contained in the particulate phase, resulting in better gas solid contact. With fluidization aids, fine

particles bed expansion improved much higher, because the cohesive property of fine particles inhibited gas flowing out of the bed. But for Geldart group A particles, nanoparticles influence on bed expansion were unobvious.

When fine particle fluidized, bed expansion keep increasing with gas velocity goes up. A new dimensionless parameter named bed height growth factor (R_G) were introduced to express particle expansion ability, and R_G is defined as the slope of BER after minimal fluidization. With the increasing additive concentration, higher bed height growth factor indicated the positive effect of nanoparticles on bed height growth.

Fine particles collapse curve were different with the typical bed collapse, a large sedimentation stage decided the high dense phase compared to Geldart group A. Superficial gas velocity was an important factor to effect dense phase bed height. But when gas velocity up a certain value, dense phase height no longer increase, this phenomenon could use to find the optimum velocity, keeping suitable dense phase.

7.2 Recommendations

Comprehensive studies have been carried out in the present work on the fundamentals of fine particle fluidization (i.e., pressure drop, bed expansion and collapse test, minimal, fluidization velocity), flowability improvement by nanoparticles as flow aids. Nevertheless, further investigations on these subjects remain necessary and recommendation are brought into attention here for more research on study and application of the fine particle fluidization technology.

- It has been realized that fluidization characterization of different kinds of particles were hard to classify and summarize, the key matter were not only the particle density,

another supposed factor was particle surface energy, there is a great deal of potential growth for both theoretical and experimental studies on surface energy effect between fine particles and nanoparticles.

- Agglomeration is usually the major problem associated with the handling of cohesive powders in industries. Nanoparticle effect on agglomerate size could be investigated, finer host particle size like sub-micron on fluidization characterization are worthy for further studied.
- As particle size management shows the improved fluidization, particle size distribution as an importance factor appears in significant influence of fluidization behavior. A huge gap between fundamental studies of fine particle fluidization and its applications or potential applications to the modern chemical, pharmaceutical and material industries still exists, so a trial experiments on simple reaction investigation in fine particle fluidized offers plenty of room for future study.

Curriculum Vitae

Name: Mengqi Han

Post-secondary Education and Degrees: East China University of Science and Technology
Shanghai, China
2010-2014, B.Eng.

The University of Western Ontario
London, Ontario, Canada
2014-2015, M.E.Sc

Honours and Awards: Western Engineering Scholarship
2014

Related Work Experience

Teaching Assistant
The University of Western Ontario
2015

Research Assistant
The University of Western Ontario
2014-2015

Publications: **To be Submitted**
Mengqi Han, Jesse Zhu, “Characterization of Fine Particle Fluidization with Nano-additives” Plan to submit to Powder Technology.